

Mathematical modeling of COVID-19 pandemic in the context of sub-Saharan Africa: a short-term forecasting in Cameroon and Gabon

C. H. NKWAYEP

*Laboratory of Mathematics, Department of Mathematics and Computer Science, University of Douala,
PO Box 24157, Douala, Cameroon
IRD, Sorbonne University, UMMISCO, F-93143, Bondy, France*

S. BOWONG*

*Laboratory of Mathematics, Department of Mathematics and Computer Science, University of Douala,
PO Box 24157, Douala, Cameroon
IRD, Sorbonne University, UMMISCO, F-93143, Bondy, France*

*Corresponding author. Email: sbowong@gmail.com

B. TSANO

*University of Dschang Task-force for the Fighting of COVID-19, Department of Mathematics and
Computer Science, University of Dschang, PO Box 67, Dschang, Cameroon
Department of Mathematics and Applied Mathematics, University of Pretoria, Pretoria 0002,
South Africa
IRD, Sorbonne University, UMMISCO, F-93143, Bondy, France*

M.A. AZIZ ALAOU

Normandie University, UNIHAVRE, LMAH, FR-CNRS-3335, ISCN, Le Havre, 76600, France

AND

J. KURTHS

*Postdam Institute for Climate Impact Research (PIK), Telegraphenberg A 31, 14412 Potsdam, Germany
Department of Physics, Humboldt Universitat zu Berlin, 12489 Berlin, Germany*

[

In this paper, we propose and analyse a compartmental model of COVID-19 to predict and control the outbreak. We first formulate a comprehensive mathematical model for the dynamical transmission of COVID-19 in the context of sub-Saharan Africa. We provide the basic properties of the model and compute the basic reproduction number \mathcal{R}_0 when the parameter values are constant. After, assuming continuous measurement of the weekly number of newly COVID-19 detected cases, newly deceased individuals and newly recovered individuals, the Ensemble of Kalman filter (*EnKf*) approach is used to estimate the unmeasured variables and unknown parameters, which are assumed to be time-dependent using real data of COVID-19. We calibrated the proposed model to fit the weekly data in Cameroon and Gabon before, during and after the lockdown. We present the forecasts of the current pandemic in these countries using the estimated parameter values and the estimated variables as initial conditions. During the estimation period, our findings suggest that $\mathcal{R}_0 \approx 1.8377$ in Cameroon, while $\mathcal{R}_0 \approx 1.0379$ in Gabon meaning that the disease will not die out without any control measures in these countries. Also, the number of undetected cases remains high in both countries, which could be the source of the new wave of COVID-19 pandemic. Short-term predictions firstly show that one can use the EnKf to predict the COVID-19 in Sub-Saharan Africa and that the second vague of the COVID-19 pandemic will still increase

in the future in Gabon and in Cameroon. A comparison between the basic reproduction number from human individuals \mathcal{R}_{0h} and from the SARS-CoV-2 in the environment \mathcal{R}_{0v} , has been done in Cameroon and Gabon. A comparative study during the estimation period shows that the transmissions from the free SARS-CoV-2 in the environment is greater than that from the infected individuals in Cameroon with $\mathcal{R}_{0h} = 0.05721$ and $\mathcal{R}_{0v} = 1.78051$. This imply that Cameroonian apply distancing measures between individual more than with the free SARS-CoV-2 in the environment. But, the opposite is observed in Gabon with $\mathcal{R}_{0h} = 0.63899$ and $\mathcal{R}_{0v} = 0.39894$. So, it is important to increase the awareness campaigns to reduce contacts from individual to individual in Gabon. However, long-term predictions reveal that the COVID-19 detected cases will play an important role in the spread of the disease. Further, we found that there is a necessity to increase timely the surveillance by using an awareness program and a detection process, and the eradication of the pandemic is highly dependent on the control measures taken by each government.

Keywords: COVID-19; mathematical model; basic reproduction number; EnKf; forecasts.

1. Introduction

On November 17, 2019, a disease appeared in a city, Wuhan, in China. Having the symptoms of an ordinary flu, it happened to be caused by a type of the coronavirus discovered in 2002 (Phelan *et al.*, 2020; Gorbalenya *et al.*, 2020). The disease spread to several cities in China and research showed that it was caused by a new coronavirus named SARS-CoV-2. It was subsequently declared as an epidemic in late December 2019 and named COVID-19 (Chan *et al.*, 2003; Li *et al.*, 2020a; Huang *et al.*, 2020). The opening of China to the outside world (with trade, tourism and others) has promoted the spread of this epidemic to other countries and on January 13, 2020, a first case was discovered outside of mainland China (Phelan *et al.*, 2020; Wang *et al.*, 2020; Chen *et al.*, 2020). The epidemic progressed on all continents and a public health emergency of international scope was declared by the World Health Organization on January 30, 2020, that this disease became the COVID-19 pandemic.

Since the appearance of the first case of COVID-19 in Cameroon on March 06, 2020 (Health, 2020), the minister of public health gave a report on the evening of July 23, 2020, according to which, out of 145 000 tests carried out, Cameroon has recorded 16 708 confirmed cases; 14 539 healed; 385 deaths; 1784 active cases and 409 hospitalized including 30 under intensive care (Manaouda, 2020). The confirmed cases would have been higher if the measures had not been taken by the Cameroonian Government. Indeed, a first state of alert was announced on March 17 with more than 13 drastic measures: wearing a mask in all areas opened to the public, intensification of the awareness campaign in urban and rural areas, the stopping of face-to-face lessons in all schools, closing leisure places after 6 p.m. and barrier methods (COVID-19 pandemic in Cameroon, 2020). On April 6, the measures became compulsory throughout the national territory. But the socio-economic impact of these drastic measures led to a fall in the gross domestic product and several households could no longer support according to the Inter-Patronal Grouping of Cameroon (Gicam) (GICAM, 2020). According to Gicam, 92% of the sampled companies declared that the COVID-19 pandemic has had a very negative (52%) or negative (40%) impact on their activities. Moreover, small and medium-sized enterprises in Cameroon (SMEs) and service companies are the most affected. The proportion of SMEs reporting a very negative impact is higher (61%) than that of large companies (27%). Similarly, 58% of service companies reported being very negatively impacted by the COVID-19 pandemic compared to 38% of industrial companies. As a result, the country may experience a loss of growth of 3% in the current economic year. The deterioration in the budgetary balance would be 2.8% and the deterioration in the current balance by 1.4%. This socio-economic situation was at the origin of the lifting of drastic measures on May 01,

2020, and the return to the classrooms on June 01, 2020, in Cameroon. After Cameroon in Central Africa, the neighboring countries began to register cases of COVID-19. For instance, on March 12, 2020, 'the Gabonese government declared the first case of COVID-19, a 27-year-old compatriot living in Gabon and having stayed in Bordeaux, France' ([Gabonactu.com, 2020](#); [UNICEF, 2020a](#)). The second case in Gabon was recorded in Bitam, a suburb in northern Gabon on April 2, 2020. It was a 32-year-old Gabonese student who returned from neighboring Cameroon following the closure of her university ([Gabonactu.com, 2020](#)). According to UNICEF, the number of COVID-19 confirmed cases in Gabon was 5087 on June 24, 2020 ([UNICEF, 2020b](#)). The increase of positive cases is compounded by the spread of the virus through the country. Moreover, on May 16, 2020, five out of the nine provinces have recorded cases and Libreville remained the major epicenter. Since the confirmation of the first case in Gabon, 6617 tests have been carried out (as of 14 May), and the country is continuously increasing its testing capacity ([UNICEF, 2020a](#)). Similar to Cameroon, on May 11, 2020, the Gabonese government lifted the state of emergency, which was enforced since April 10, 2020. In addition, the Government opted for the easing of Libreville and surrounding areas. However, the curfew is still in place to prevent the spread of the SARS-CoV-2 in Gabon. In addition, key guidelines were issued for public places, these include the following: mandatory wearing of face masks, strict hand-washing and use of sanitizers, observance of physical distancing and ban on public gathering; ban of passenger flights (both national and international); ban of inter-provincial commuters; school closure. The partial and total confinement in certain provinces in Gabon has considerably influenced the evolution of COVID-19 as this country recorded on July 19, 2020: 6315 confirmed cases; 3865 healed; 46 deaths and 2404 active cases ([Politologue.com, 2020](#)). However, it is possible that the pandemic continue to spread throughout the World and WHO declared on July 21, 2020, being able to end the COVID-19 pandemic in less than 'two years'. Therefore, several studies need to be done to help each government to apply the best control measures in the process of fighting the COVID-19 pandemic.

Mathematical tools are used to understand several evils that plague societies today. Numerous compartmental models have been implemented to complete the epidemiology and statistical analysis in order to prevent and control epidemics ([Fung, 2014](#); [Bowong & Kurths, 2010](#); [Chao *et al.*, 2014](#); [Eikenberry *et al.*, 2020](#)). As in the study of many other infectious diseases, modeling efforts on COVID-19 have mainly focused on mean-field compartmental models, either deterministic or stochastic, as well as agent-based models ([Eikenberry *et al.*, 2020](#); [Ranjan, 2020](#); [Nadim *et al.*, 2021](#); [Guan *et al.*, 2020](#); [Lin *et al.*, 2020](#); [Zhou *et al.*, 2020](#); [Chowdhury *et al.*, 2020](#); [Li *et al.*, 2020b](#); [Verity *et al.*, 2020](#); [Roda *et al.*, 2020](#); [Tang *et al.*, 2020](#); [Nkwayep *et al.*, 2020](#)). Despite the difficulty in understanding the evolution of the new SARS-CoV-2 at this time, most studies on epidemiological observations and hypotheses have been done ([Ranjan, 2020](#); [Nadim *et al.*, 2021](#); [Guan *et al.*, 2020](#); [Fei *et al.*, 2020](#)). Some results indicate that there are indirect contaminations through the environment and direct contaminations human to human and others still discuss for aerosol transmission of the SARS-CoV-2 ([WHO, 2020a](#)). In order to understand and control COVID-19 in a human population, several researchers have proposed different models of transmission of the new SARS-CoV-2 ([Lin *et al.*, 2020](#); [Giordano *et al.*, 2020](#); [Li *et al.*, 2020c](#); [Prem *et al.*, 2020](#); [Saldaña *et al.*, 2020](#)). However, a large majority of these works does not take into account the fact that a sensitive human can also contract the SARS-CoV-2 through an indirect transmission by contact with free in the environment ([Adhikari *et al.*, 2020](#)). During an epidemic, when human-to-human and virus-to-human transmissions are established and reported cases rised worldwide, forecasting is of utmost importance for health care planning and control of the virus with limited resources.

In the fitting process of an epidemic, it is important to have some information that help either to create better control or to predict the future of the epidemic. For this, it is important to design a model

that will help to reconstruct some of unknown past information based on the present information. The data are used to find or reconstruct these information that we call estimated states and parameters. Since its inception in the 1960s for the estimation of states in linear system, the Kalman Filter (*KF*) has undergone different improvements and today we can estimate the states and parameters even of non-linear systems (Kailath *et al.*, 2000; Bras & Rodriguez-Iturbe, 1994; Zheng *et al.*, 2009; Gillijns *et al.*, 2006a). The Extended Kalman filter (*EKf*) proceeds by adopting the formula of the classical Kalman filter with the Jacobian of the dynamics matrix (in both continuous and discrete time) playing the role of the linear dynamics matrix (Gillijns *et al.*, 2006a), but this would increase estimation errors. The Ensemble Kalman Filter (*EnKf*) belongs to a broader category of filters known as particle filters (Gillijns *et al.*, 2006a; Kotecha & Djuric, 2003). Unlike (*EKf*) estimation and unscented Kalman filter estimation, particle filters use neither the Jacobian of the dynamics nor frozen linear dynamics. In the case of the unscented Kalman filter (Wan & Merwe, 2000), the number of sample points required is equal to the dimension of the system. On the other hand, the number of ensembles required in the (*EnKf*) is heuristic. While one would expect that a large ensemble would be needed to obtain appropriate estimates, the literature on *EnKf* suggests that an ensemble of 50 to 100 points is often adequate for systems with thousands of states (Gillijns *et al.*, 2006a). With the complexity of many phenomena, the estimation of both of states and parameters for dynamical systems are of high interest. *EnKf* has successfully dealt with this issue (Bourgeois *et al.*, 2011; Narula *et al.*, 2016).

Several mean-field compartmental models have been recently formulated to calibrate COVID-19 mathematical models through either least square or Monte Carlo Markov Chain (MCMC) (Zhou *et al.*, 2020; Chowdhury *et al.*, 2020; Li *et al.*, 2020b; Verity *et al.*, 2020). Micheal Li et al. (Roda *et al.*, 2020) used MCMC to estimate the parameters related to COVID-19 transmission in China. They presented the trends of the epidemic in the same country and show why it is difficult to predict the COVID-19. Tang *et al.* (2020) introduced control strategies in the human transmission to estimate the basic reproduction number in Wuhan, but the proposed model cannot take into account the circulation of free SARS-CoV-2 viruses in the environment. In Song *et al.* (2021), an extended Kalman filter has been developed to estimate the COVID-19 spread based on SEIRD model. In a recent paper Nkwayep *et al.* (2020), an *EnKf* approach has been used to fit the data of COVID-19 pandemic in Cameroon using a SIR-type model with the incorporation of indirect transmission. The trends of the pandemic are given when different control strategies are applied.

This paper has been motivated by the following epidemiological question. *With the evidence of free-living SARS-CoV-2 in the environment, can the number of undetected COVID-19 cases for the ongoing outbreak be more accurately estimated?* The estimation of COVID-19 undetected cases has been considered recently in Liu *et al.* (2021); Griette *et al.* (2020); Maugeri *et al.* (2020); Liu *et al.* (2020); Rocchetti *et al.* (2020); Perkins *et al.* (2020); Barbarossa *et al.* (2020). However, these works didn't take into account the circulation of free coronaviruses in the environment and the effect of awareness programs. To answer the above-raised research question, we develop here the *EnKf* approach for the estimation of unmeasurable state variables and unknown parameters using real data of the current COVID-19 pandemic in Cameroon and Gabon. We first formulate a mathematical model for the transmission dynamics of COVID-19 pandemic in the context of Sub-Saharan Africa. The proposed model includes the following four important epidemiological features. (i) The circulation of free SARS-CoV-2 viruses in the environment. (ii) The compliance to preventive methods against COVID-19 through awareness programs. (iii) The stigmatization and ignorance of some COVID-19 patients who do not present themselves for screening after the appearance of first symptoms. (iv) The non-pharmaceutical interventions such as mass media-based sensitization, social distancing, face-mask wearing, contact tracing and the disinfection and decontamination of infected places by using suitable

products against free SARS-CoV-2 in the environment. We study the basic properties of the model, such as the positivity of the solutions and the boundedness of the trajectories. We compute the disease-free equilibrium and derive the basic reproduction number \mathcal{R}_0 that determines the outcome of the COVID-19 pandemic when parameter values are constant. Then, we assume that the weekly number of newly COVID-19 detected cases, deceased and recovered cases are accessible to measurements but that COVID-19 transmission rates, detection rate of undetected cases, recovery and deceased rates are unknown time-dependent parameters. Then, we use the *EnKf* method to investigate both states and parameters estimation in the formulated model. We apply this estimation method to real weekly data of the current COVID-19 pandemic from March 6, 2020 to April 11, 2021 in Cameroon and March 13, 2020, to February 21, 2021, in Gabon (Politologue.com, 2020; WORLDDOMETER, 2020). Data have been grouped in week in order to obtain the same observations in all web sites where the data of COVID-19 in Cameroon and Gabon have been published rather than in days where small differences have been observed and to better observe the evolution of the COVID-19 in over a large period. This has permitted to estimate the number of COVID-19 undetected cases, the concentration of free SARS-CoV-2 circulating in the environment, the real total number of COVID-19 cases and the estimated values of unknown parameters. Then, we use the mean values of the estimated parameters during the period that data have been collected to compute the basic reproduction number \mathcal{R}_0 both in Cameroon and Gabon. We find that $\mathcal{R}_0 \approx 1.8377$ in Cameroon, while $\mathcal{R}_0 \approx 1.0379$ in Gabon. We observe that during the considered period, the number of COVID-19 undetected cases and the concentration of free SARS-CoV-2 viruses in the environment have increased and have played an important role in the spread of the disease. We did a short-term forecasts of the pandemic using the estimated initial conditions of model and compared the results to the reported data from April 11, 2021, to July 04, 2021, in Cameroon and from February 21, 2021, to April 04, 2021, in Gabon. In addition, we used these results to extend the forecast of COVID-19 pandemic until July 10, 2022, in Cameroon and until April 03, 2022, in Gabon. We have found that the COVID-19 pandemic can disappear in Cameroon before the two years deadline predicted by WHO with the current riposte enacted by the government since the lockdown. However, this pandemic may remain endemic in Gabon for a longer period of time if the Gabonese health system will not be enhanced in the meantime. Unlike many studies on mathematical modeling of COVID-19 in the world and in particular in sub-Saharan Africa ([Eikenberry et al., 2020](#); [Ranjan, 2020](#); [Nadim et al., 2021](#); [Guan et al., 2020](#); [Lin et al., 2020](#); [Zhou et al., 2020](#); [Chowdhury et al., 2020](#); [Li et al., 2020b](#); [Verity et al., 2020](#); [Roda et al., 2020](#); [Tang et al., 2020](#); [Nkwayep et al., 2020](#); [Liu et al., 2021](#); [Griette et al., 2020](#); [Maugeri et al., 2020](#); [Liu et al., 2020](#); [Rocchetti et al., 2020](#); [Perkins et al., 2020](#); [Barbarossa et al., 2020](#)), our study includes the non-detection of some COVID-19 cases due to many reasons, such as the stigmatization, the use of traditional African pharmacopoeia, the ignorance of the negative effects of this pandemic, the circulation of free SARS-CoV-2 viruses in the environment, the recklessness, the ignorance and the poverty of some individuals who do not respect any preventive methods against COVID-19, which is usually the case in sub-Saharan Africa where some individuals are still illiterate.

The paper is organized as follows. In Section 2, we present the material and methods. Section 3 gives the main results of the work. The last section is devoted to the discussions and concluding remarks.

2. Materials and Methods

2.1 A COVID-19 transmission model in the context of sub-Sahara Africa

Herein, we formulate a mathematical model for the dynamical behavior of the current COVID-19 pandemic in the context of sub-Sahara Africa. We consider a compartmental differential equation

model for the dynamical transmission of COVID-19 where we adopt a variant that reflects some key epidemiological and biological properties of COVID-19 in sub-Saharan Africa. The model is based on the following assumptions. (i) We consider some demographic effects by assuming a proportional natural death rate in each of the sub-populations of the model. In addition, our model includes a net inflow of susceptible individuals into the region or country, which includes new births and immigration. Indeed, in many countries of Sub-Saharan Africa, the number of COVID-19 induced mortality is much lower than the number of new birth so that it is not very realistic to neglect the demographic in modeling of COVID-19. (ii) In reality, awareness programs, like any other educational efforts, are limited by available resources and many other socioeconomic factors, and it is usually impossible for these programs to reach the entire host population. As a result, people who are involved in the awareness programs will be more informed about the spread and severity of the disease and will be more likely to make efforts to avoid catching the disease. In contrast, those individuals who are not reached by the awareness programs will likely lack knowledge of the disease and will possibly make no change of their daily life, so that they will be at higher risk for contracting the disease. (iii) COVID-19 detected cases can infect susceptible individuals. Due to the limited number of beds in some hospitals, patients with COVID-19 who do not need respiratory assistance will take their treatment at home and will thus be able to continue to infect those around them. Also, COVID-19 hospitalized individuals may infect the health care personal who lack adequate personal protective equipment. (vi) Some COVID-19 undetected cases will recover from the infection by taking medicines from the African traditional pharmacopoeia. Indeed, WHO recognizes that traditional, complementary and alternative medicine has many benefits and Africa has a long history in traditional medicine and practitioners that play an important role in providing care to populations. Medicinal plants such as *Artemisia annua* are being considered as possible treatments for COVID-19 and should be tested for efficacy and adverse side effects (Ekonde, 2020; WHO, 2020b). WHO is working with African research institutions to select traditional medicine products that can be investigated for clinical efficacy and safety for COVID-19 treatment (WHO, 2020b; Kapepula *et al.*, 2020).

The population under consideration is grouped into disjoint classes or compartments. We divide the human population into five states representing disease status. At any time t , there are the following epidemiological classes.

- (i) Unaware susceptible individuals $S_u(t)$: This class contains individuals who are susceptible to COVID-19 and do not comply to preventive methods against COVID-19 or individuals who still have no knowledge about the disease. Unaware individuals may switch to the aware group due to compliance to preventive methods through awareness programs, and aware susceptible individuals who fail to comply to preventive methods against COVID-19 may become unaware susceptible individuals.
- (ii) Aware individuals $S_a(t)$: The class of aware susceptible individuals comprises individuals who are susceptible to COVID-19 and observe the COVID-19 preventive methods against COVID-19 such as the social distancing, the mask-face wearing, the use of hydro-alcoholic gel the washing of hands with soap and the disinfection of surfaces every time. Individuals in the S_a compartment have lower chances of contracting the disease than those in S_u compartment (Ghosh & Martcheva, 2021).
- (iii) COVID-19 undetected individuals $I_u(t)$: The class of COVID-19 undetected cases comprises those who have been exposed to free SARS-CoV-2 in the environment and who have not been detected or suspected by the authorities in charge of COVID-19. This class also comprises

asymptomatic and symptomatic cases. As in COVID-19 detected cases, COVID-19 undetected cases comprise asymptomatic and symptomatic infected individuals. Indeed, the increased number of COVID-19 undetected cases is associated with the social stigma associated with COVID-19. In fact, when talking about COVID-19, certain words (i.e. suspect case, isolation...) and language may have a negative impacts on people and fuel stigmatizing attitudes. These undesirable attitudes can perpetuate existing negative stereotypes or assumptions, strengthen false associations between the disease and other factors, create widespread fear or dehumanize those who have the disease (UNICEF, 2020c). This can drive people away from getting screened, tested and quarantined.

- (iv) COVID-19 detected individuals $I_d(t)$: The class of COVID-19 detected cases comprises all those persons who at some point were considered exposed cases and a confirmatory laboratory test has been conducted to confirm that there is indeed an infection with SARS-CoV-2. This class of COVID-19 infected cases comprises asymptomatic (exposed individuals who were exposed to the virus but clinical signs of COVID-19 have not yet developed) and symptomatic individuals (exposed individuals who present the clinical symptoms of COVID-19). In fact, many data of the current COVID-19 pandemic in sub-Saharan Africa do not distinguish asymptomatic and symptomatic infected individuals.
- (v) Recovered individuals $R(t)$: This class comprises detected and undetected cases that recover from the infection. As suggested by many studies in the literature, recovered individuals may only have partial immunity (Hui *et al.*, 2020a; Kampf *et al.*, 2020). Indeed, there is no evidence that recovered individuals of COVID-19 acquire a permanent immunity. That is, just because an individual recovers from the virus does not mean he/she cannot catch it again. Indeed, on 24 April, the World Health Organization (WHO) in a statement said ‘there is currently no evidence that people who have recovered from COVID- 19 and have antibodies are protected from a second infection’ (WHO, 2021). So, we assume that recover will progress in an aware susceptible after a certain period of time corresponding to the mean duration of time they will spend before losing their acquired immunity.

Thus, the total human population at time t is

$$N(t) = S_u(t) + S_a(t) + I_d + I_u(t) + R(t). \quad (1)$$

The complexity of the COVID-19 into human population resides in the ability of free coronaviruses to live in the environment. According to some studies (Kampf *et al.*, 2020; Hui *et al.*, 2020b), the virus can remain viable in the environment between 12 hours and 9 days depending on the temperature. Then, we consider in this work the free coronaviruses living in the environment and we denote it by $V(t)$.

Unaware susceptible individuals are recruited into the human population at rate Λ . Unaware susceptible individuals gain knowledge of the disease and enter the S_a class through awareness programs at a rate ρ . Meanwhile, aware individuals become unaware of the disease over time and enter the S_u class at a rate γ . We assume that the observation to preventive methods against COVID-19 may reduce but not completely eliminate susceptibility to infection. For this reason, we consider a factor η as the efficacy of the compliance to preventive methods against COVID-19. When $\eta = 1$, the compliance is perfect while, $\eta = 0$ means that the compliance has no effect at all. Thus, the value $1 - \eta$ can be understood as the inefficacy level of the compliance to preventive methods.

A transmission of COVID-19 occurs due to adequate contacts between susceptible individuals, COVID-19 detected cases and undetected cases and free SARS-CoV-2 concentration in the environment.

We consider that, even if the detected individuals are isolated, they can also contribute to the human infection through nosocomial transmission (Hussen & Alemu, 2021; Fouogue *et al.*, 2020). We assume that the transmission of COVID-19 disease from COVID-19 infectious to susceptible individuals is modelled by a standard incidence, while the transmission of COVID-19 disease from the free coronaviruses in the environment to exposed individuals is modelled by the Holling type II function. Unaware and aware susceptible individuals can be infected by SARS-Cov-2 after adequate contacts with COVID-19 infected cases and free SARS-Cov-2 in the environment at rates $\lambda(I_d, I_u, V)S_u$ and $(1 - \eta)\lambda(I_d, I_u, V)S_a$, respectively, where $\lambda(I_d, I_u, V)$ is the force of infection modelled by

$$\lambda(I_d, I_u, V) = \frac{\beta_d(t)I_d(t) + \beta_u(t)I_u(t)}{N} + \beta_v(t)\frac{V(t)}{K + V(t)}. \quad (2)$$

In (2), $\beta_d(t)$ and $\beta_u(t)$ are the COVID-19 transmission rates from detected and undetected cases, respectively, and $\beta_v(t)$ the COVID-19 transmission rates from free SARS-CoV-2 in the environment which are assumed to be time-dependent.

Due to significant variations in the control strategies, which change over time, we consider control measures that reduce the time-varying COVID-19 transmission rates to minimal values by taking into account non-pharmaceutical interventions. Without loss of generality, we assume that at time t , some governments can decide to take control measures in order to reduce the transmission rates β_d , β_u and β_v to minimal values $\beta_{h,min}$ and $\beta_{v,min}$. Thus, similar to Tang *et al.* (2020), the COVID-19 transmission rates are modeled as follows:

$$\begin{aligned} \beta_d(t) &= \beta_{h,min} + (\beta_{h,0} - \beta_{h,min})e^{-r_d t}, & \beta_u(t) &= \beta_{h,min} + (\beta_{u,0} - \beta_{h,min})e^{-r_u t} \\ \text{and} \quad \beta_v(t) &= \beta_{v,min} + (\beta_{v,0} - \beta_{v,min})e^{-r_v t}. \end{aligned} \quad (3)$$

In Eq. (3), $\beta_{d,0}$ is the mean value of the contact rate at time t without COVID-19 and $\beta_{v,0}$ is the mean value of contact rate between human individuals and free SARS-CoV-2 viruses in the environment without COVID-19. The constants r_d , r_u are the decay rate of human contacts due to barrier measures, face-masks wearing, washing hands with soap and regular use of hydro-alcoholic gels. On the other hand, the constant r_v is the decay rates of contacts between human and free SARS-CoV-2 in the environment due to the disinfection and decontamination of infected places.

After contracting the infection at rate $\lambda(I_d, I_u, V, t)$, a proportion p of unaware susceptible individuals is detected and enters the class of COVID-19 detected case at rate $p\lambda(I_d, I_u, V, t)S_u$, while the remainder is not detected and is transferred in to the class I_u of COVID-19 undetected cases. Also, among aware susceptible individuals who contracted the new coronavirus, a proportion q is detected at rate $q(1 - \eta)\lambda(I_d, I_u, V, t)S_a$ and enters the class of COVID-19 detected cases, while the remainder $(1 - q)(1 - \eta)\lambda(I_d, I_u, V, t)S_a$ is undetected and transferred in to the class I_u . We assume that COVID-19 undetected individuals can recover naturally. At each time, COVID-19 undetected cases are suspected or detected or recovered at rate ω . However, a proportion δ of ω are suspected or detected by the authorities in charge of COVID-19 and enter the class of COVID-19 detected cases and the rest $(1 - \delta)\omega$ recover. The COVID-19 detected cases recover from the disease after a therapeutic treatment at rate θ . The classes of COVID-19 detected and undetected cases are affected by COVID-19 induced mortality at rates d_d and d_u , respectively. Humans in the S_a , S_u , I_d , I_u and R classes succumb naturally at rate μ , where $1/\mu$ is approximately the lifespan of humans. The COVID-19 detected and undetected cases shed SARS-CoV-2 viruses in the environment at rates ξ_d and ξ_u , respectively. Finally, the free SARS-CoV-2 in the environment die at rate ν . As suggested by many studies, recovered individuals may only

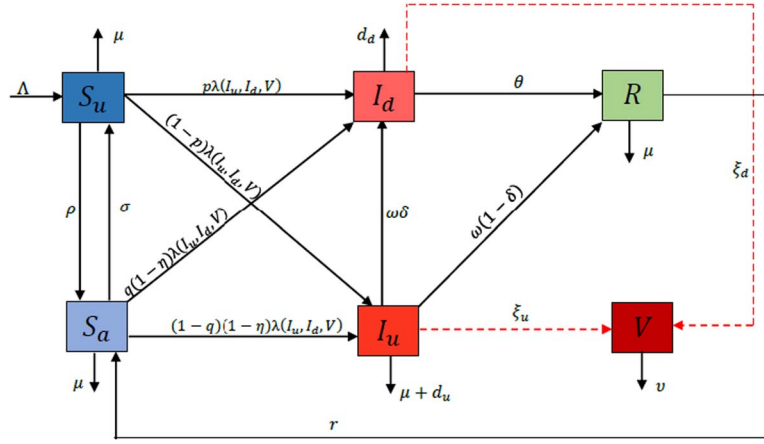


FIG. 1. Structure of the model.

have partial immunity (Hui *et al.*, 2020a; Kampf *et al.*, 2020; Mbopi-Keou *et al.*, 2020). Indeed, there is no evidence that recovered individuals of COVID-19 acquire a permanent immunity. That is, just because an individual recovers from the virus does not mean he/she cannot catch it again. Indeed, on 24 April, the World Health Organization (WHO) in a statement said ‘there is currently no evidence that people who have recovered from COVID-19 and have antibodies are protected from a second infection’ (World Health Organisation (WHO), 2021).

The flowchart of the whole model is presented in Fig. 1. The solid lines represent the flows between human compartments, the dashed lines represent the shedding of virus in the environment and the curved dashed lines stand from new infectious coming from the interaction of susceptible individuals with the environment.

Using the flowchart in Fig. 1, the COVID-19 transmission model is expressed by the following system of differential equations:

$$\begin{cases} \dot{S}_u = \Lambda + \gamma S_a - (\lambda(I_u, I_d, V, t) + \rho + \mu) S_u, \\ \dot{S}_a = \rho S_u + r R - ((1 - \eta) \lambda(I_u, I_d, V, t) + \gamma + \mu) S_a, \\ \dot{I}_d = (p S_u + q(1 - \eta) S_a) \lambda(I_u, I_d, V, t) + \omega \delta I_u - (d_d + \theta + \mu) I_d, \\ \dot{I}_u = ((1 - p) S_u + (1 - q)(1 - \eta) S_a) \lambda(I_u, I_d, V) - (\delta + \omega + d_u + \mu) I_u, \\ \dot{R} = \theta I_d + \omega(1 - \delta) I_u - (r + \mu) R, \\ \dot{V} = \xi_u I_u + \xi_d I_d - \nu V. \end{cases} \quad (4)$$

Tables 1 and 2 summarize, respectively, the model variables and the parameter values used for numerical simulations of system (4).

2.2 Ensemble Kalman filter approach

Here, we present the ensemble Kalman filtering approach Gillijns *et al.* (2006a) for the dual estimation of state variables and parameters.

TABLE 1 *Variables with units for system (4).*

Symbols	Description	Units
S_u	Unaware susceptible individuals	<i>Individual</i>
S_a	Aware susceptible individuals	<i>Individual</i>
I_d	COVID-19 detected cases	<i>Individual</i>
I_u	COVID-19 undetected cases	<i>Individual</i>
R	Recovered individuals	<i>Individual</i>
V	Free SARS-CoV-2 concentration in the environment	<i>Cell</i>

For this, we consider a first equation of an epidemiological model given by

$$\dot{x}(t) = g(x(t), \phi(t), u(t)), \quad (5)$$

where x represents the state variables with appropriate dimension. $\phi(t)$ a vector of unknown parameters that one can model as a Markov process and u is considered as a control. Finally, the observations of phenomena are $h(x(t), \phi(t))$.

Then, the estimation problem with the Ensemble Kalman filter considers the following system:

$$\begin{cases} x_{t+1} = f(x_t, \phi_t, u_t) + w_t, \\ \mathcal{Y}_t = h(x_t, \phi_t) + \psi_t, \\ \phi_{t+1} = \phi_t + \sigma_t, \end{cases} \quad (6)$$

where $x_t \in \mathbb{R}^n$ is the state variables given after discretization of the continuous system (5). The observation that depends the states and the parameters $\phi_t \in \mathbb{R}^p$ is denoted by $y_t \in \mathbb{R}^m$. In Eq. (6), w_t , v_t and σ_t are white noises with the covariance matrices Q_t , S_t and R_t , respectively.

The estimation procedure of the state variables x_t and parameters ϕ_t for system (6) is given in Appendix A.

3. Results

In this section, we show how the estimation method proposed in the previous section can be used to calibrate system (4) using real data of the current COVID-19 pandemic in Cameroon and Gabon.

3.1 Basic properties

Herein, we study the positivity and boundedness of solutions of system (4). Clearly, the right hand side of system (4) is a C^∞ function. Thus, according to the Cauchy–Lipschitz theorem a unique maximal solutions exist for any initial condition. Moreover, the following result holds.

THEOREM 3.1 System (4) is a dynamical system on the biologically feasible compact domain:

$$\Omega = \left\{ (S_u, S_a, I_d, I_u, R, V) \in \mathbb{R}_+^6, N(t) \leq \frac{\Lambda}{\mu}, V(t) \leq \frac{(\xi_d + \xi_u)\Lambda}{\nu\mu} \right\}. \quad (7)$$

The proof of Theorem 3.1 is given in Appendix B.

TABLE 2 Definition and values of the parameters for system (4).

Symbols	Description	Value/range	Reference
Λ	Human recruitment rate	$indiv. week^{-1}$	Perspective Monde (2020)
μ	Natural mortality rate for human	$week^{-1}$	Perspective Monde (2020)
β_{d0}	COVID-19 transmission rate of detected cases without interventions	$[0, 1] week^{-1}$	To be estimated
β_{u0}	COVID-19 transmission rate of undetected cases without interventions	$[0, 1] week^{-1}$	To be estimated
β_{v0}	COVID-19 transmission rate of free SARS-CoV-2 in the environment without intervention	$[0, 1] week^{-1}$	To be estimated
r_d	Decay rate of detected contacts	$[0, 1] week^{-1}$	To be estimated
r_u	Decay rate of undetected contacts	$[0, 1] week^{-1}$	To be estimated
r_v	Decay rate of human contacts with free SARS-CoV-2 in the environment	$[0, 1] week^{-1}$	To be estimated
d_d	COVID-19 detected induced mortality rate of detected cases	$[0, 1] week^{-1}$	To be estimated
θ	Recovery rate of COVID-19 detected cases	$[0, 1] week^{-1}$	To be estimated
ω	Transfer rate of COVID-19 undetected cases	$[0, 1] week^{-1}$	To be estimated
δ	Proportion of COVID-19 undetected cases who are detected	$[0, 1] week^{-1}$	To be estimated
p	Proportion of unaware susceptible individuals that become newly COVID-19 detected cases	$[0, 1]$	To be estimated
q	Proportion of aware susceptible individuals that become newly COVID-19 detected cases	$[0, 1]$	To be estimated
ν	Decrease rate of free SARS-CoV-2 in the environment	$1/2 week^{-1}$	Renwick (2020)
ξ_d	Shedding rate of SARS-CoV-2 detected cases in the environment	$0.01 cells.(week. indiv)^{-1}$	Renwick (2020)
ξ_u	Shedding rate of SARS-CoV-2 undetected cases in the environment	$0.5 cells.(week. indiv)^{-1}$	Renwick (2020)
η	Efficacy of preventive methods against COVID-19	0.9180	Assumed
ρ	Rate at which unaware susceptible individuals become aware susceptible individuals	$0.0255 week^{-1}$	Assumed
σ	Rate at which aware susceptible individuals become unaware susceptible individuals	$0.015 week^{-1}$	Assumed
d_u	COVID-19 induced mortality rate of undetected cases	$0.028 week^{-1}$	Assumed
K	Positive constant	$10^6 cells$	Assumed
r	Rate of loss of immunity in recovered individuals	$7/90 week^{-1}$	Business Today (2021); Support the Guardian (2021)

We compute the basic reproduction number \mathcal{R}_0 of system (4) in the case when that all parameters of the model are constants, i.e. $\beta_d(t) = \beta_d$ and $\beta_v(t) = \beta_v$. The basic reproduction number is the average number of secondary cases produced by a single infective individual, which is introduced into an entirely susceptible population (Van den Driessche & Watmough, 2002).

System (4) has a disease-free equilibrium $X_0 = (S_u^0, S_a^0, 0, 0, 0, 0)$ obtained by setting the right-hand side of equations in system (4) to zero with $I_u = I_d = 0$:

$$X_0 = \left(\frac{(\gamma + \mu)\Lambda}{(\rho + \gamma + \mu)\mu}, \frac{\rho\Lambda}{(\rho + \gamma + \mu)\mu}, 0, 0, 0, 0 \right)^T. \quad (8)$$

Using the next generation matrix approach (Van den Driessche & Watmough, 2002), the basic reproduction number of system (4) when all the parameters are constant is

$$\mathcal{R}_0 = \mathcal{R}_{0h} + \mathcal{R}_{0v}, \quad (9)$$

where

$$\mathcal{R}_{0h} = \frac{\beta_h}{N^0} \left[\frac{\varepsilon S^0}{d_d + \theta + \mu} + \left(\frac{\omega\varepsilon}{d_d + \theta + \mu} + 1 \right) \frac{C^0}{\delta + \omega + d_u + \mu} \right] \quad (10)$$

and

$$\mathcal{R}_{0v} = \frac{\beta_v}{(d_d + \theta + \mu)Kv} \left(\xi_d S^0 + \frac{(\xi_u(d_d + \theta + \mu) + \xi_d\omega)C^0}{\delta + \omega + d_u + \mu} \right), \quad (11)$$

with

$$S^0 = pS_u^0 + q(1 - \eta)S_a^0, \quad C^0 = (1 - p)S_u^0 + (1 - q)(1 - \eta)S_a^0,$$

$$S_u^0 = \frac{(\gamma + \mu)\Lambda}{(\rho + \gamma + \mu)\mu} \quad \text{and} \quad S_a^0 = \frac{\rho\Lambda}{(\rho + \gamma + \mu)\mu}.$$

We refer the reader to Appendix for the computation of the basic reproduction number of system (4).

Biologically speaking, if $\mathcal{R}_0 \leq 1$, we are sure that the COVID-19 pandemic will disappear, while if $\mathcal{R}_0 > 1$, it will persist within the community. After the estimation of the unknown parameters in the next section, we will estimate the value of \mathcal{R}_0 in order to predict the outcome of pandemic. Indeed, we plan to estimate the unknown parameters each week and use the mean values of these estimated parameters to estimate the basic reproduction number \mathcal{R}_0 .

3.2 States space formulation with *EnKf* using data

Herein, we present an estimation method for the reconstruction of unmeasurable state variables and the unknown parameters of system (4) by means of *EnKf* (Moradkhani *et al.*, 2005). We also use the parameter estimates to subsequently estimate the value of the basic reproduction number. The goal of this step is to shed light on the epidemic since the beginning by estimating some unknown state variables and parameters. Furthermore, using these state variable estimates as initial conditions and unknown parameters, we give the short-term forecasts of COVID-19 pandemic. Note that this prediction is very

useful to control and prevent the spread. The advantage of the dual estimation is that the estimated state is mined for the estimation of the parameters, which preserves the stability of the estimation [Bourgeois et al. \(2011\)](#); [Gillijns et al. \(2006\)](#).

The estimation problem is formulated via recurrent equations on the states and the parameters to be estimated. In addition to these equations, the observations of the system are used as inputs to the system. For system (4), all the states are not directly observed. According to data of the current COVID-19 pandemic in Sub-Saharan Africa, the only measurement available online (or ‘observation’) concerns the weekly number of detected cases, the weekly number of deceased individuals and the weekly number of recovered individuals. This is quite reasonable from an epidemiological point of view: the weekly number of detected cases is rather easy to be detected or suspected and counted by the authorities in charge of COVID-19. Once they are detected, they are isolated and undergo treatment so that some of them will recover or die if the treatment fails. We assume that the measurable outputs of system (4) are the newly COVID-19 detected cases given by

$$(pS_u(t) + q(1 - \eta)S_a(t))\lambda(I_u, I_d, V, t) + \delta\omega I_u(t),$$

newly recovered individuals

$$\theta I_d(t)$$

and newly deceased

$$d_d I_d(t).$$

The measurable variables of the COVID-19 model (4) denoted by $\mathcal{Y}(t)$ is then modeled as follows:

$$\mathcal{Y}(t) = \begin{pmatrix} (pS_u(t) + q(1 - \eta)S_a(t))\lambda(I_u, I_d, V, t) + \omega I_u(t) \\ \theta I_d(t) \\ d_d I_d(t) \end{pmatrix} + \psi_t, \quad (12)$$

where $\psi_t \in \mathbb{R}^3$ is the white noise that is assumed to be a Gaussian distribution with deviation Z_t . We point out that ψ_t can be interpreted as the error appearing when the data of the COVID-19 cases are reported by the health authorities.

Even if the recovery rate θ and the deceased rate d_d are known, in more realistic situations, several uncertainties may appear. The rate of screening $\delta\omega$ of undetected cases is unknown. For instance, the force of infection is not well known. Indeed, the transmission rate from COVID-19 infected cases β_d and β_u and free SARS-CoV-2 in the environment β_v are uncertain. Thus, the transmission rates β_d , β_u and β_v are considered as unknown parameters in system (4) and need to be estimated. To achieve this, we estimate the average contact rates β_{d0} , β_{u0} and β_{v0} and the efficacy rates r_d , r_u and r_v linked to the barrier measures used to cope with the evolution of the new coronavirus. Also, we estimate the proportions p and q of the newly detected unaware and aware cases, respectively. The unknown parameters at time t are $\phi_t = (\beta_{d0,t}, \beta_{u0,t}, \beta_{v0,t}, r_{d,t}, r_{u,t}, r_{v,t}, d_{d,t}, \theta_t, p_t, q_t, \omega_t, \delta_t)$ and can be written in a simple state space model following a Markov process:

$$\phi_{t+1} = \phi_t + \sigma_t, \quad (13)$$

where σ_t is the uncertainty at time t given by a Gaussian white noise in \mathbb{R}^9 with standard deviations T_t . In fact, σ_t can be interpreted as the behavior changes influence on the transmission rates that grow or fall beyond a certain limits 0 and 1.

Finally, we simulate system (4) using the Runge–Kutta method. Since each variable of system (4) follows a Markov process (Bourgeois *et al.*, 2011; Narula *et al.*, 2016), we use the following discrete model:

$$x_{t+1} = f(x_t, \phi_t) + w_t, \quad (14)$$

where w_t is the incertitude at time t of the discretization (error) that is assumed to be a white noise process with the covariance matrix Q_t that appreciates the estimation of the exact value of the state variables $x(t) \equiv x_t = (S_u(t), S_a(t), I_d(t), I_u(t), R(t), V(t))^T$. The function $f(x_t, \phi_t)$ is the approximated value of x_{t+1} given by the discrete model obtained by discretizing system (4) using the Runge–Kutta method.

Herein, we use the EnKf procedure (Bourgeois *et al.*, 2011) to estimate the states x_t and the parameters ϕ_t for each data \mathcal{Y}_t using the following system:

$$\begin{cases} x_{t+1} = f(x_t, \phi_t) + w_t, \\ \mathcal{Y}_t = h(x_t, \phi_t) + \psi_t, \\ \phi_{t+1} = \phi_t + \sigma_t, \end{cases} \quad (15)$$

where

$$h(x_t, \phi_t) = ((p_t S_u(t) + q_t(1 - \eta)S_a(t))\lambda(I_u, I_d, V, t) + \delta_t \omega_t I_u(t), \theta_t I_d(t), d_{d,t} I_d(t))^T.$$

We apply the Kalman Ensemble filtering process described in the Appendix A to system (15) in order to estimate unmeasurable states and unknown parameters of COVID-19 pandemic in Cameroon and Gabon. We point out that five parameters have been hypothetically based on the results of the sensitivity analysis of the model and numerical tests. Indeed, all parameters contained in the force of infection can be estimated using the EnKf approach. To our best knowledge, there is no way to estimate the parameters that are not contained in the force of infection using the EnKf approach.

3.3 Error of estimation

Now, to assess the accuracy of the short-term forecasts, we calculate two performance metrics, namely the mean absolute error (MAE) and the root mean square error (RMSE) defined using a set of performance metrics as follows:

$$\text{MAE} = \frac{1}{n} \sum_{i=1}^n |Y(i) - \widehat{Y}(i)|, \quad (16)$$

and

$$\text{RMSE} = \sqrt{\frac{1}{n} \sum_{i=1}^n |Y(i) - \widehat{Y}(i)|^2}, \quad (17)$$

where $Y(i)$ represent the data, $\widehat{Y}(i)$ are the forecasts values and n is the size of the predicted data.

3.4 Study case of the current COVID-19 epidemic in Cameroon

Here, we show how the estimation method developed in the previous section can be used to reconstruct the unmeasurable state variables and unknown parameters using real data of the current COVID-19 pandemic in Cameroon. For numerical simulations, we take the parameter values given in Table 2. The covariance matrices of the error are chosen according to the evolution process of each to be estimated. The deviations are chosen to be $Q_t = 0.2I_6$, $T_t = 10^{-5}\mathcal{I}_{12}$ and $Z_t = \text{diag}(0.015, 0.001, 0.001)\mathcal{I}_3$. We use the COVID-19 real data from March 08, 2020, to July 04, 2021, in Cameroon (Politologue.com, 2020; WORLDOMETER, 2020) for the calibration of system (4). We point out that the Cameroonian government is still collecting daily data for the COVID-19 pandemic. In the present study, we consider the following three periods: (i) the first period concerns starts from the beginning of the pandemic when no preventive measures is applied going from March 08, 2020, to April 05, 2020. (ii) The second period corresponds to the period when control measures such as lockdown of people, non-pharmaceutical interventions such as mass media-based sensitization, social distancing, face-mask wearing, contact tracing and the disinfection and decontamination of infected places using suitable products against free SARS-CoV-2 in the environment in order to reduce the spread of the disease have been recommended by the Cameroonian government, from April 06, 2020, to May 03, 2020, and (iii) the third period corresponds to the period when the lockdown of people is put in place, from May 04, 2020, to July 04, 2021.

Figure 2 presents the weekly reported data of the number of newly COVID-19 detected cases, newly recovered individuals and newly deceased during each period (magenta, blue and red lines). We point out that the data have been grouped in weeks in order to have the same data in all web sites where the data of COVID-19 in Cameroon and Gabon have been published and to better observe the evolution of COVID-19 in these countries.

3.4.1 Model validation. Herein, we process with the validation of system (4) using real data of Fig. 2. To do so, system (15) was simulated with the following initial condition: (26425825, 0, 2, 10, 1, 700), so that $S_u(0) + S_a(0) + I_d(0) + I_u(0) + R(0)$ assumes the total population of Cameroon at the beginning of the pandemic. We choose $\mu = 17562$ and $\Lambda = 3.261 \cdot 10^{-4}$ Perspective Monde (2020). We use real data given in Fig. 2 and the *EnKf* procedure for the reconstruction of both the state variables and unknown transmission rates. The results of numerical simulations are depicted in Figs 3–6.

Figure 3 gives the estimation of the transmission rates. The reconstruction of the parameter values (β_{d0} , β_{u0} , β_{v0} , r_d , r_u and r_v) of the transmission rates are given in Fig. 3, while Fig. 4 presents the reconstruction of parameters, which influence the propagation of the COVID-19 pandemic. It is θ , d_d , ω , p , q and δ . The reconstruction of transmission rates given in Eq. (3) are depicted in Fig. 5(a)–(c). One can observe that at the beginning of COVID-19 in Cameroon (the first four weeks), contacts between susceptible and either detected cases or undetected cases show a moderate increase, while contacts between susceptible individuals and free SARS-CoV-2 in the environment have decreased (see the magenta lines in Fig. 3(a)–(c) and in Fig. 5(a)–(c)). The results also show that at the beginning of the epidemic in Cameroon, among susceptible individuals who did not take preventive measures against the disease, about 1.3% of the newly infected individuals were detected each week and approximately 34.4% of people complied the preventive methods against COVID-19. Thus, more individuals who contracted COVID-19 were not detected, i.e. 98% and 65% of unaware and aware individuals, respectively. At the same period, one observes that more than 80% of undetected cases were detected (see the magenta lines in Fig. 4(d)–(f)). One can observe that during the lockdown, the screening campaign have increased (see the blue lines in Fig. 4(c) and (f)), while the other proportions did not vary too much. However,

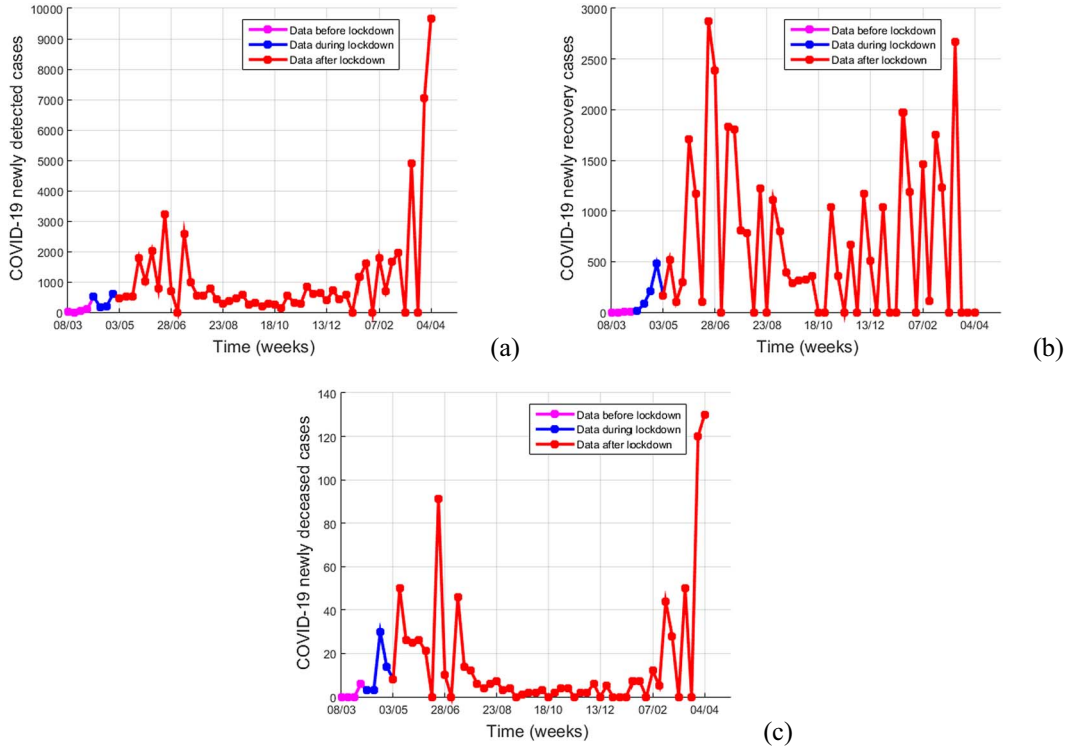


FIG. 2. Reported data of COVID-19 from 08-03-2020 to 04-04-2021 in Cameroon. [Politologue.com \(2020\)](#); [WORLDOMETER \(2020\)](#). (a) Newly infected cases, (b) newly recovered individuals and (c) newly deceased.

after the lockdown (third period), we note a sharp decrease in the proportion of newly aware infected and strong decrease of newly unaware infected even if it still less the 10%. An increasing of screening of detection of undetected cases (see the red lines in Fig. 4(c)–(f)). We also note an increase in all the transmission rates immediately after the lockdown, but the transmission rate β_d started to decrease while the transmission β_u and β_v involved around 0.01 and 0.02, respectively (see the red lines in Fig. 5(a)–(c)). An increase has been observed in the cure rate, but the lethal rate remains than 0.2% during the lockdown (see the blue lines in Fig. 4(a) and (b)). Also, after the lockdown the decay rates r_d and r_u increased, while the decay rates r_v increased firstly and decreased after (see the red lines in Fig. 3(d)–(f)). This induced a decreasing of the transmission rates from either the detected individuals β_d or the undetected ones β_u (see the red line in Fig. 5(a) and (b)). But, it induced an increasing of contact between susceptible individuals and free SARS-CoV-2 in the environment β_v (see the red line in Fig. 5(c)). To add further evidence of these results, we fit the basic reproduction number since the beginning of COVID-19 in Cameroon using the estimated values of parameters. The results is plotted in Fig. 5(d).

Figure 6 presents the results of the estimated states of system (4). We find that the free SARS-CoV-2 in the environment increase progressively during the beginning of the pandemic to reach the peak around June 21, 2020 (see Fig. 6(f)). It also illustrates that less than 3 million individuals obeyed the preventive measures against COVID-19 (see Fig. 6(b)) and that more than 24 million of susceptible individuals are still unaware at the date of April 04, 2021 (see Fig. 6(a)).

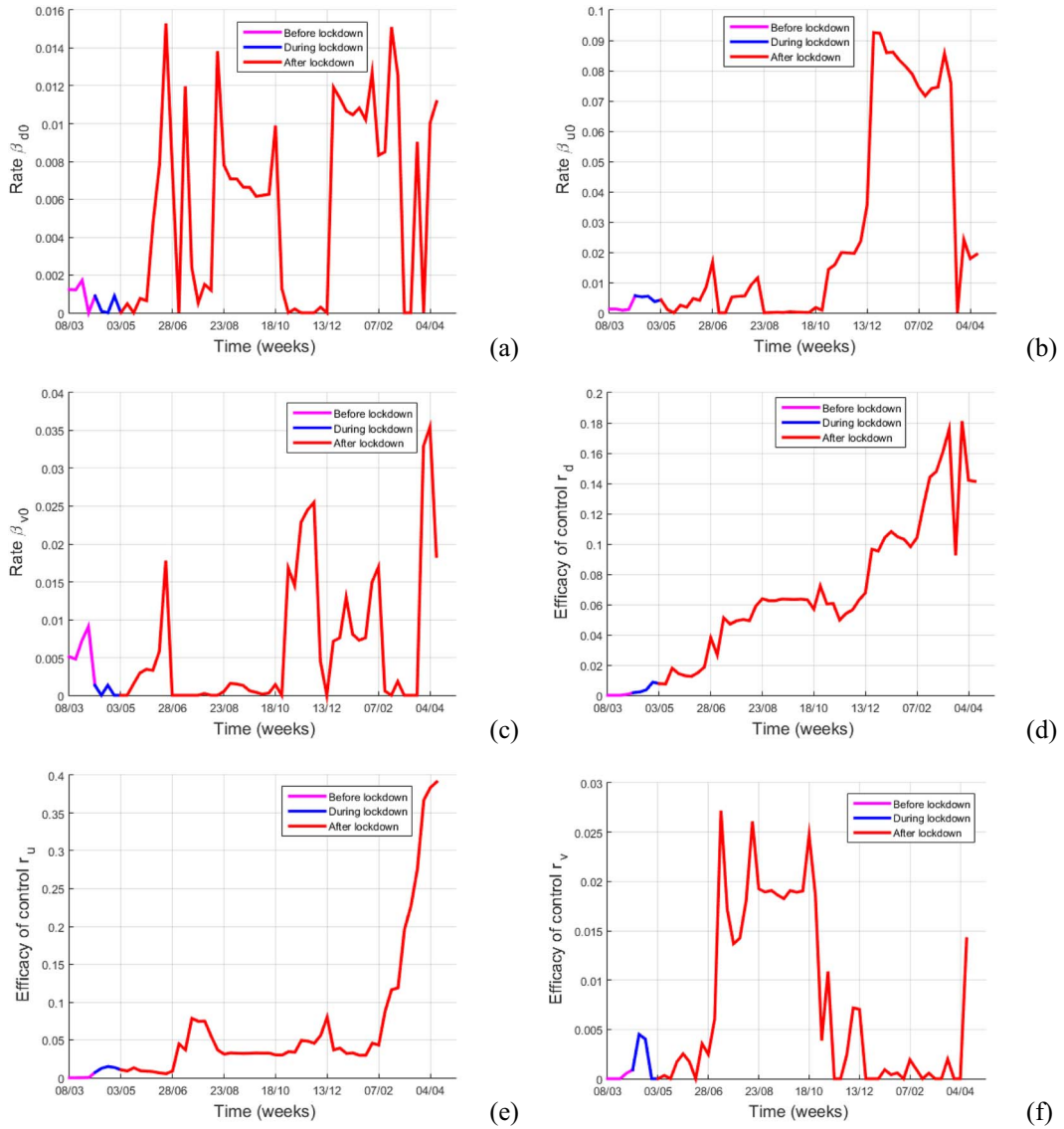


FIG. 3. Estimation of the transmission rates in Cameroon from March 08, 2020, to April 04, 2021. (a) Transmission rate from detected cases without interventions β_{d0} . (b) Transmission rate from undetected cases without interventions β_{u0} . (c) Transmission rate from free SARS-CoV-2 in the environment without intervention β_{v0} . (d) Decay rate of human contacts with detected cases r_d . (e) Decay rate of human contacts with undetected cases r_u and (f) decay rate of human contacts with free SARS-CoV-2 in the environment r_v .

Now, we use the estimated values of state variables and parameters of system (4) during the three considered periods (before, during and after the lockdown) to fit the COVID-19 data in Cameroon. The results of numerical simulations are presented in Fig. 7. The observed data are shown in magenta before the lockdown, in blue during the lockdown and in red after the lockdown. From this figure, it is evident

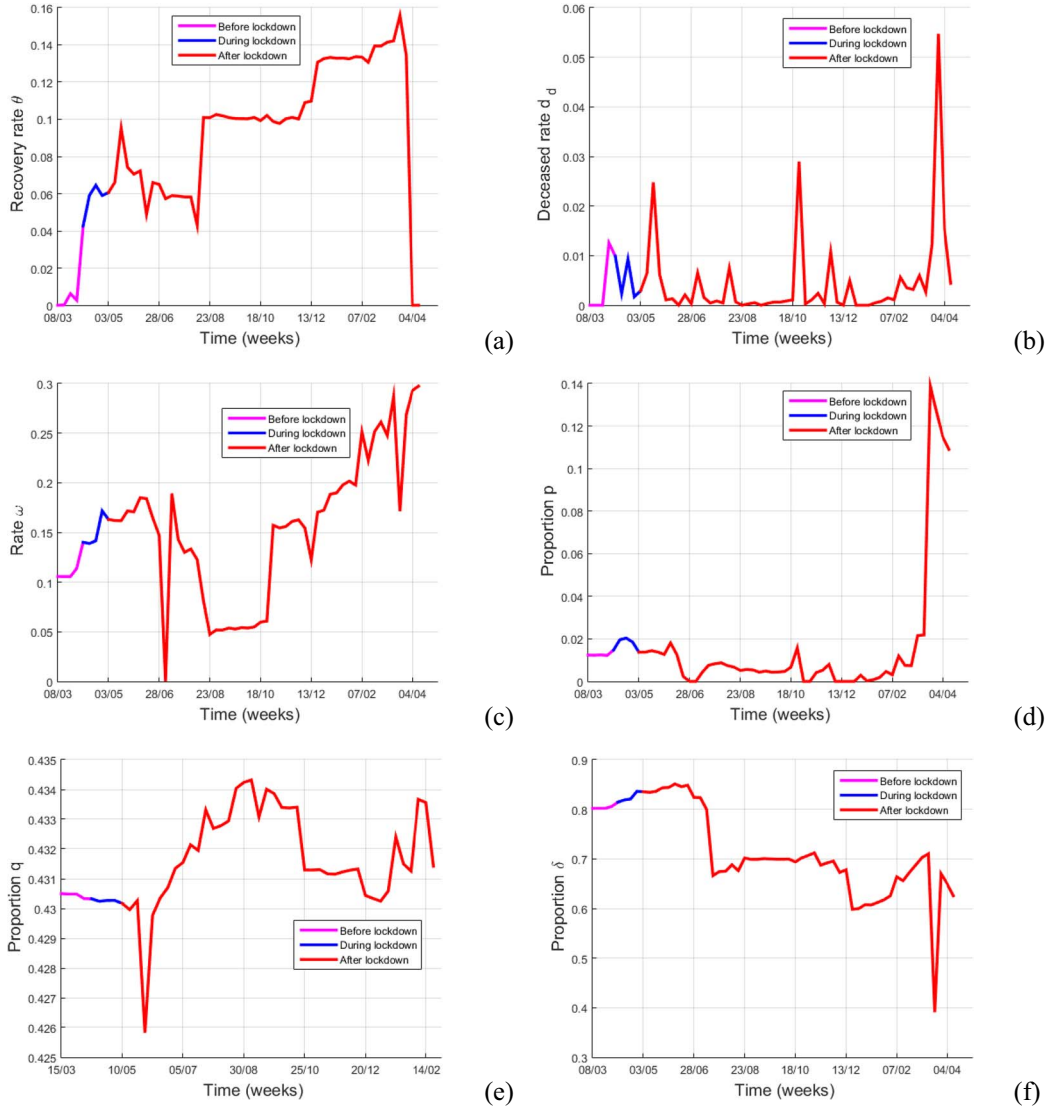


FIG. 4. Estimation of unknown parameters of COVID-19 pandemic in Cameroon using the initial conditions (26425825, 0, 2, 10, 1, 700) and the initial parameters (0.00123, 0.00123, 0.0051, 0, 0, 0, 0, 0, 0.01238, 0.344, 0.1058, 0.802). (a) Recovery rate θ ; (b) deceased rate d_d ; (c) screening rate ω ; (d) proportion p ; (e) proportion q and (f) proportion δ .

that data (star cloud) show a better fit of the estimated number of newly detected cases; newly deceased cases; newly recovery cases; active detected cases and cumulative detected cases (green lines) as shown in Fig. 7(a)–(e). The values of variables of system (4) that we estimated at April 04, 2021, are reported in Table 3.

Next, we use the estimated values of states and parameters of system (4) to estimate the number of newly undetected cases, the number of active undetected cases, the cumulative undetected cases, the total

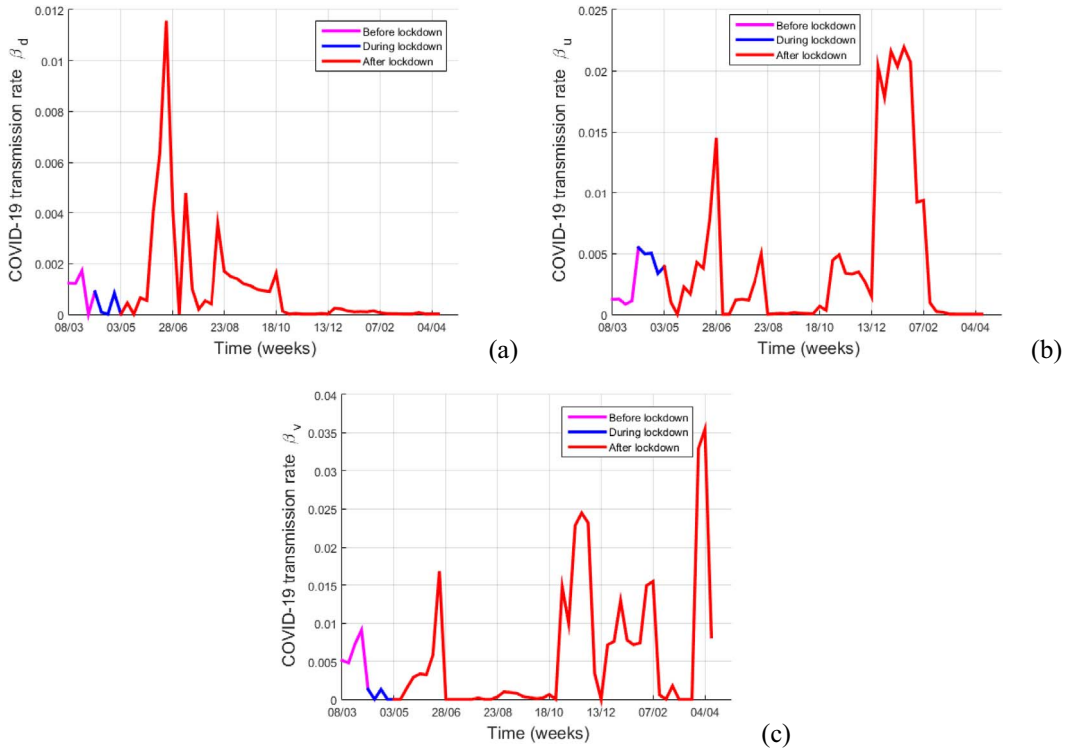


FIG. 5. Estimation of transmission rates in Cameroon since the beginning of COVID-19 until on April 04, 2021, using the estimated values of unknown parameters. (a) Transmission rate from detected cases β_d , (b) transmission rate from undetected cases β_u and (c) transmission rate from free SARS-CoV-2 in the environment β_v .

number of newly cases, the total number of active COVID-19 cases and cumulative cases in Cameroon. The results of our numerical simulations are depicted in Fig. 8. It turns out that, even if some of these individuals are either detected or recovered, others continue to transmit COVID-19 within the population (see the curve of active COVID-19 cases in Fig. 8(b)). Also, we fit the total cases in Cameroon by adding the detected and undetected cases. The result is plotted in Fig. 8(d)–(f). All these curves imply that, after the relaxation of the control measures, the pandemic started to increase rapidly as shown the red line in Fig. 8(a)–(f), Fig. 3(a)–(f), Fig. 4(c)–(f) and Fig. 5(a)–(c). Also, it is trivial that during the same period, the concentration free SARS-CoV-2 in the environment significantly increased but, started to decrease (see the red line in Fig. 6(f)). To close this part, we present the summary of cases in Cameroon at the date of April 04, 2021, in Table 4 and give the mean values of the estimated parameters of system (4) in Table 5. With these parameter values, the estimated mean value of basic reproduction number during the estimation period is $\mathcal{R}_0 \approx 1.84$. The fact that \mathcal{R}_0 is greater than one means that the COVID-19 pandemic will not die out quickly without control measures that aim at bringing this basic reproduction number below one.

3.4.2 *Forecast of COVID-19 pandemic in Cameroon.* The estimate goal of the analysis here is to present the forecasts of the current COVID-19 pandemic in Cameroon using the values of the estimated

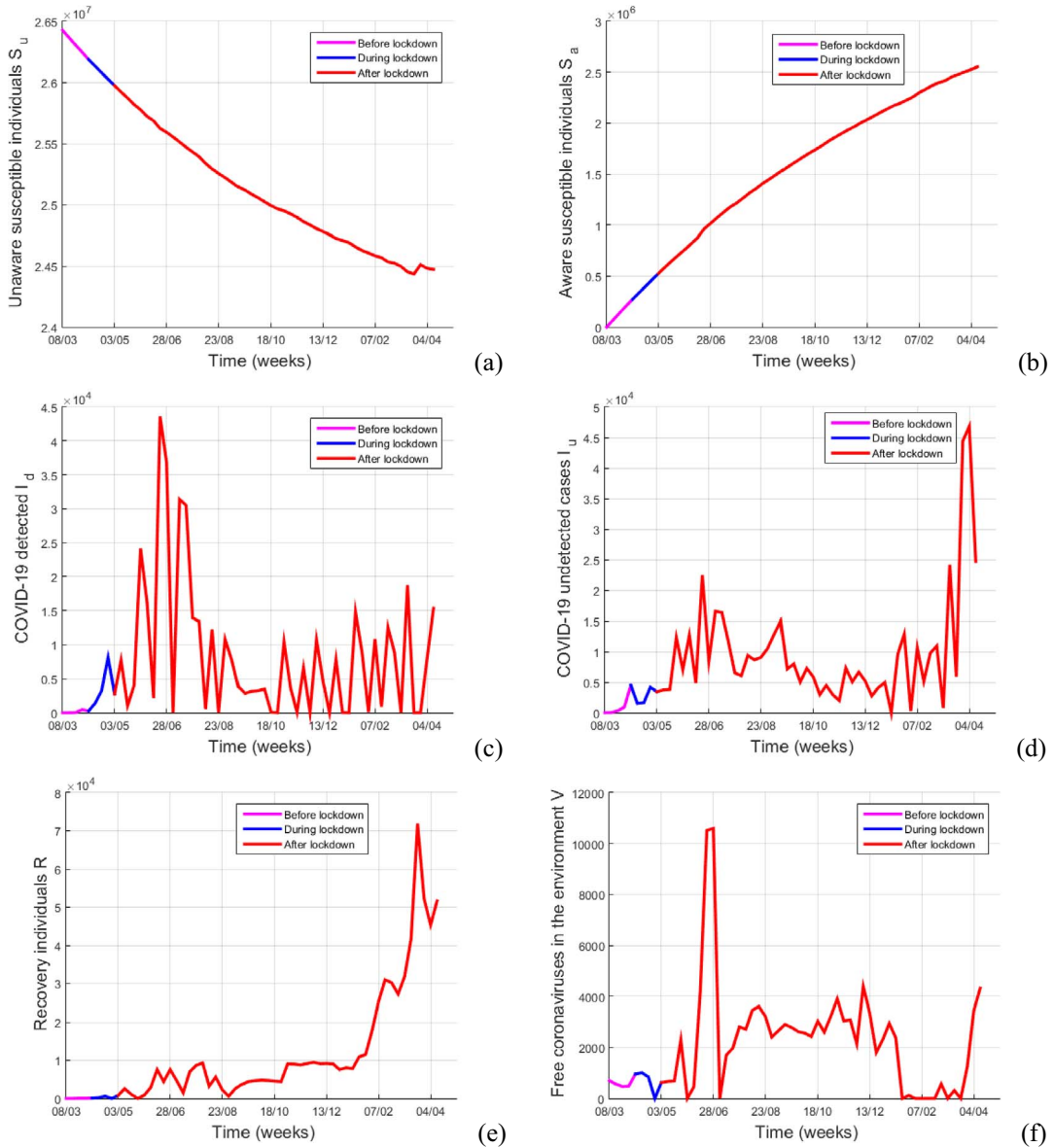


FIG. 6. Estimation of unmeasurable states of COVID-19 pandemic in Cameroon using the initial condition $(26425825, 0, 2, 10, 1, 700)$ and the initial parameters $(0.00123, 0.00123, 0.0051, 0.074, 0, 0, 0, 0, 0.001238, 0.344, 0.1058, 0.802)$ (a) Unaware susceptible individuals S_u ; (b) aware susceptible individuals S_a ; (c) detected cases I_d ; (d) undetected cases I_u ; (e) recovered individuals R and (f) free SARS-CoV-2 viruses in the environment V .

parameters and state variables in the previous sections. To achieve this, we consider the values of state variables given in Table 3 as the initial condition of system (4). Also, we use the values of parameters displayed in Table 5. We also show how the *EnKf* can be use to make short-term prediction of the

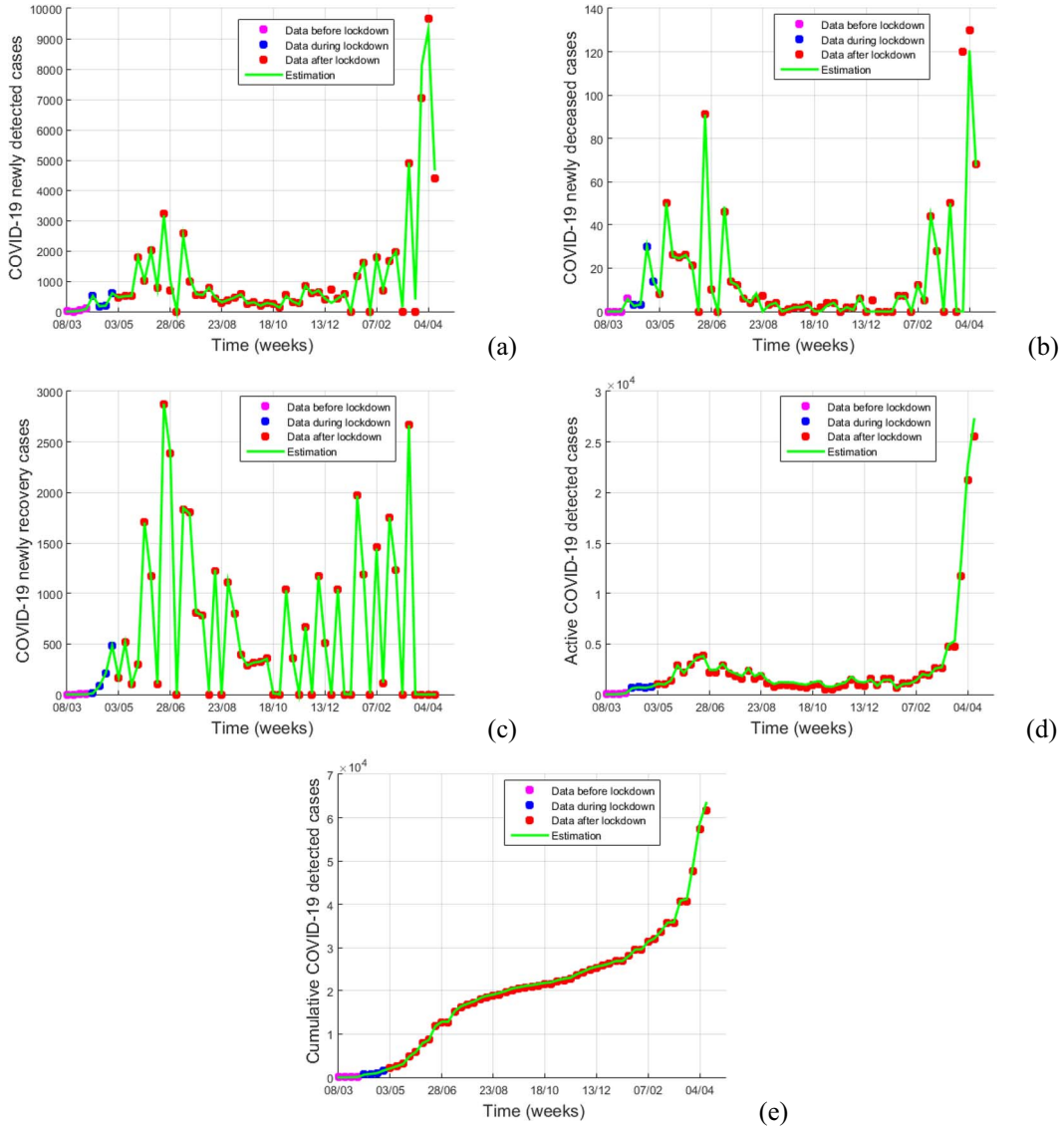


FIG. 7. Fitting results of the current COVID-19 pandemic in Cameroon using the estimated value of the transmission rates β_h and β_v given in Fig. 4 and the estimated value of state variables given in Fig. 6. (a) Newly detected cases; (b) newly deceased cases; (c) newly recovery cases; (d) active detected cases and (e) cumulative detected cases.

COVID-19 pandemic in Cameroon. For this we fitted the value obtain without used the data and the real data from April 04, 2021, to July 04, 2021.

Figures 9–11 present the forecast of COVID-19 in Cameroon from April 04, 2021, to May 29, 2022. In Fig. 9, the start points represent the data, the green lines are the estimation given by using the data in the EnKf and the blue lines represent the forecasts of the current pandemic that we fitted without data.

TABLE 3 Estimated values of state variables of system (4) in Cameroon on April 04, 2021.

Variables	S_u	S_a	I_d	I_u	R	V
Values	24 471 162	2 552 835	15 326	24 694	51 664	4 320

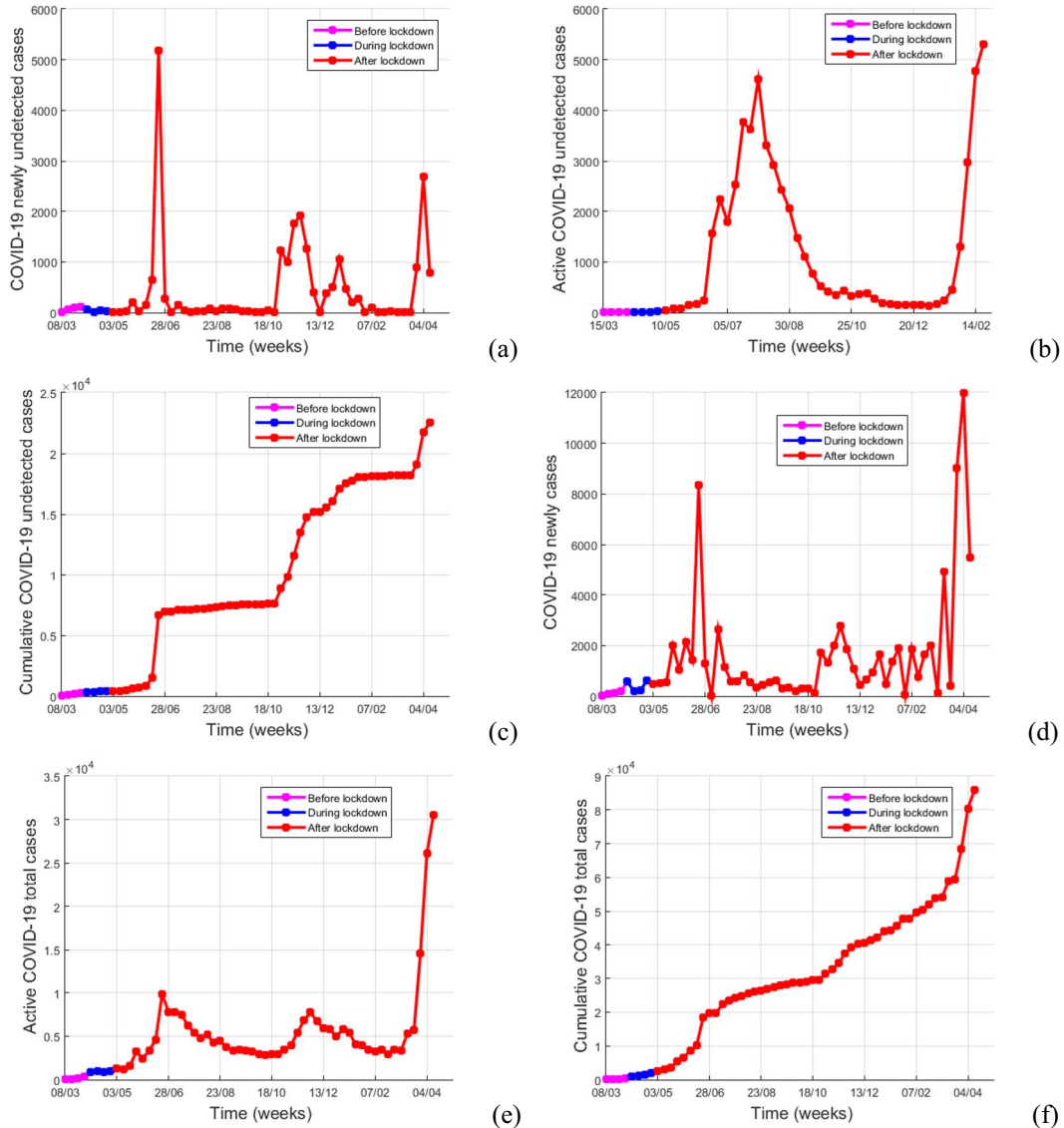


FIG. 8. Reconstruction of COVID-19 undetected cases in Cameroon using the estimated values of both states and parameters of system (4) given in Figs 3–6. (a) Newly undetected cases, (b) active undetected cases, (c) cumulative undetected cases, (d) total newly cases, (e) total active cases and (f) total cumulative cases.

TABLE 4 States of COVID-19 in Cameroon on April 04, 2021.

Variables	Detected cases		Undetected cases		Total cases	
	Active	Cumulative	Active	Cumulative	Active	Cumulative
Values	21 220	61 173	3 195	24 475	24 415	85 650

TABLE 5 Mean values of estimated parameters of the COVID-19 pandemic in Cameroon on April 04, 2021.

Parameters	Values	Parameters	Values
β_{d0}	0.008	β_{u0}	0.0215
β_{v0}	0.01235	r_d	0.1030
r_u	0.2298	r_v	0.0105
d_d	0.0045	θ	0.0428
p	0.0631	q	0.3695
ω	0.02259	δ	0.6708
β_d	0.0005	β_u	0.0021
β_v	0.0055	\mathcal{R}_0	1.8377

The results show insure that one can use the well done estimation to predict the spread of the COVID-19 in Cameroon (see the red line of forecasts obtained and the real data). The trends show that the second wave of COVID-19 is already underway in Cameroon (see red and blue line in Fig. 10(a)–(d)) and it is possible that the pandemic disappears rather quickly in Cameroon. In fact, even if \mathcal{R}_0 is greater than unity ($\mathcal{R}_0 \approx 3$), but among the human individuals it remains very close to it on April 04, 2021, ($\mathcal{R}_{0h} = 0.05$); thus compliance with barrier measures should very quickly bring the basic reproduction number below unity and gradually reduce the daily number of new infected cases (see the blue line in Fig. 9(a) and (d) , Fig. 10(a)–(d)). Note that the newly deceased will decrease progressively (see the red line in Fig. 11(a)). Also, it illustrates that the majority of COVID-19 patients will recover from the disease (see the red line in Fig. 9) and that susceptible individuals will have continuous education about the prevent of the SARS-CoV-2 in Cameroon (see the red line in Fig. 11(b)). The expected trend of COVID-19 in Cameroon at July 10, 2022, is reported on Table 6.

3.5 A study case of the current COVID-19 epidemic in Gabon

As in Cameroon case, we use the EnKf to reconstruct the unmeasurable state variables and unknown parameters using real data of the current COVID-19 pandemic in Gabon. For numerical simulations, we use the known parameter values given in Table 2. The covariance matrices of the error are chosen according to the evolution process of each object to be estimated. The deviations are chosen to be $Q_t = 0.2\mathcal{I}_6$, $T_t = 10^{-5}\mathcal{I}_{12}$ and $Z_t = 0.015\mathcal{I}_3$. We use the COVID-19 real data from March 15, 2020, to April 04, 2021, in Gabon UNICEF (2020a) for the calibration of system (4) and we consider the following three periods: (i) the first period concern starts from the beginning of the pandemic when no preventive measures is applied, from March 15, 2020, to April 12, 2020. (ii) The second period corresponds to the period when preventive measures is applied by the Gabonese government, from April 13, 2020, to May 10, 2020, and(iii) the third period corresponds to the period when the measures

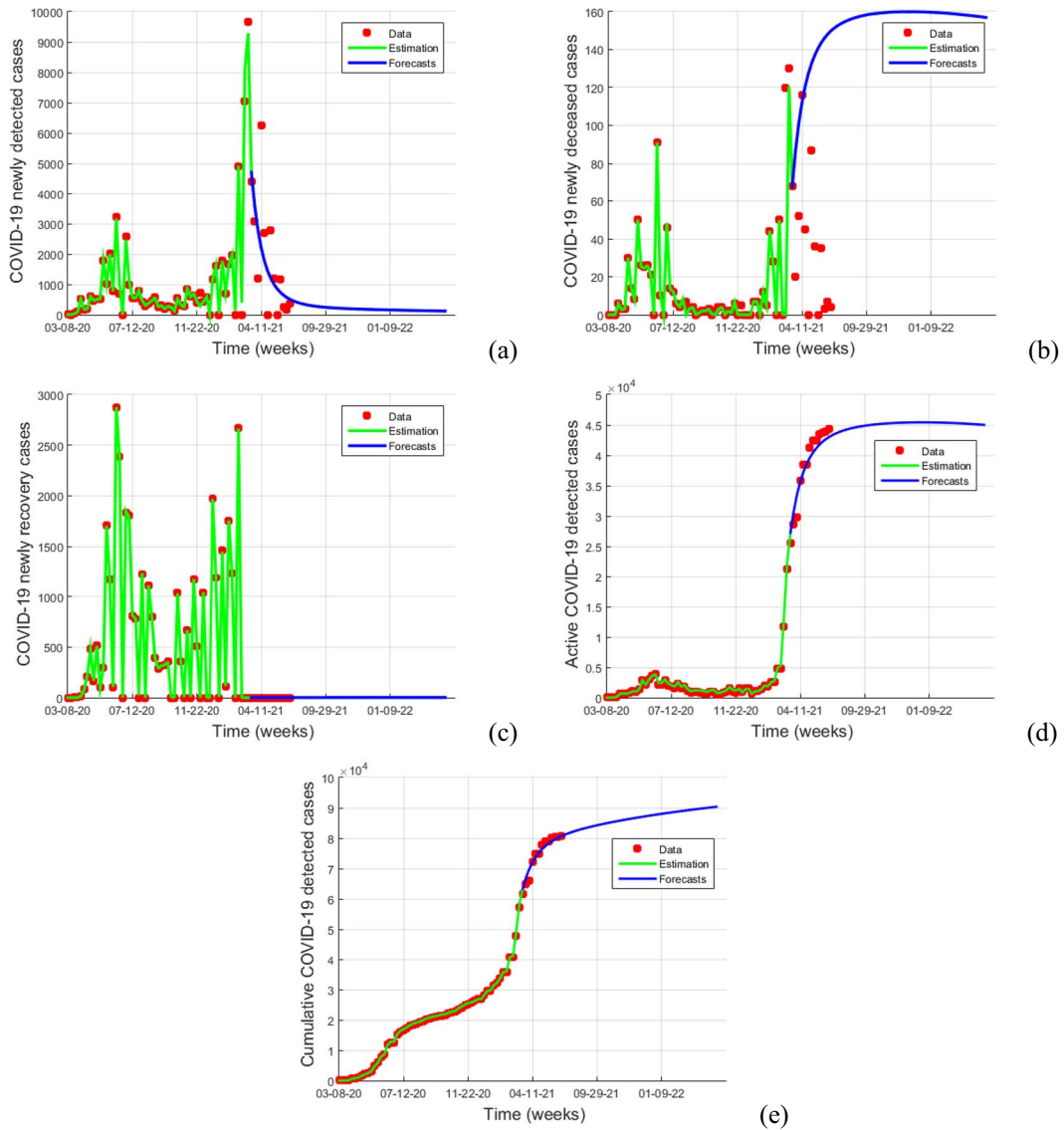


FIG. 9. Short-term forecasting of newly and active cases of COVID-19 pandemic in Cameroon. (a) COVID-19 newly detected cases; (b) COVID-19 newly deceased; (c) COVID-19 newly recovery COVID-19; (d) active COVID-19 detected cases and (e) cumulative COVID-19 detected cases.

have been relaxed in Gabon, from May 11, 2020, to February 21, 2021. The two last periods correspond to the time that the Gabonese government applied and relaxed preventive measures as in the Cameroon case.

Figure 12 presents the weekly number of newly COVID-19 detected cases, recovered individuals and deceased during each period (magenta, blue and red lines).

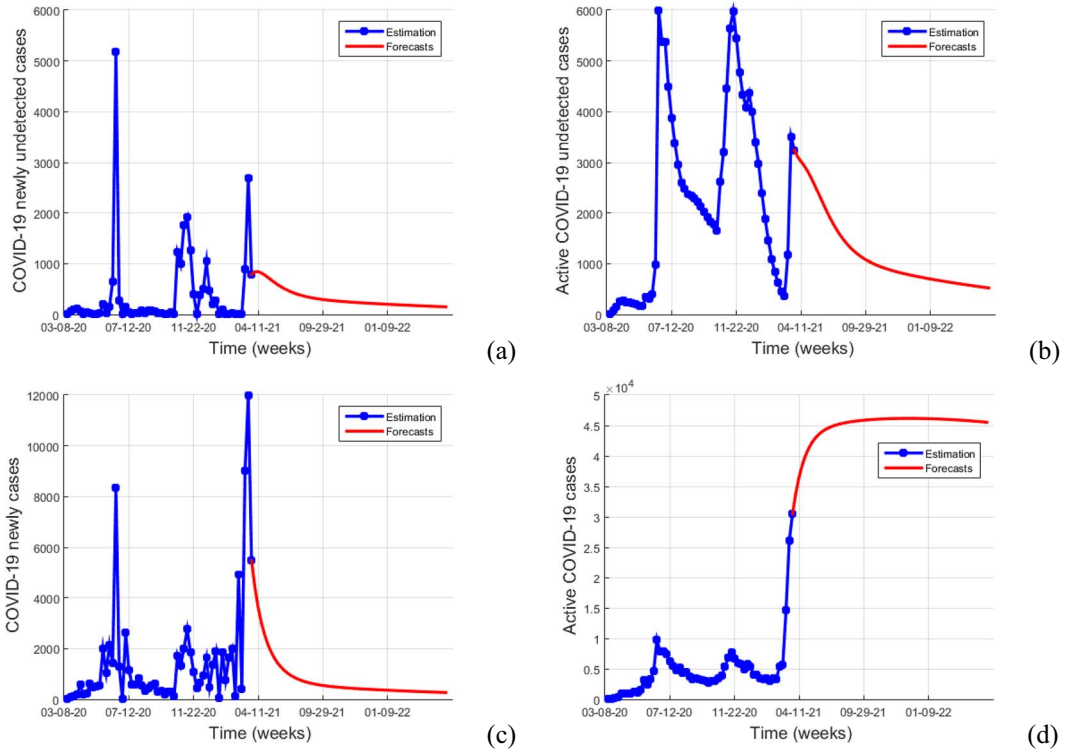


Fig. 10. Short term forecasting of newly and active cases of COVID-19 pandemic in Cameroon. (a) COVID-19 newly undetected cases; (b) active COVID-19 undetected cases; (c) COVID-19 newly cases and (d) active COVID-19 cases.

3.5.1 *Model calibration.* Herein, we process with the calibration of system using real data of COVID-19 in Gabon given in Fig. 12. System (15) was simulated with the following initial condition: (2183590, 0, 1, 5, 0, 700), so that $S_u(0) + S_c(0) + I_d(0) + I_u(0) + R(0)$ assumes the total population of Gabon at the beginning of estimate with $\mu = 1/(66.47 * (365/7))$ and $\Lambda = 1312$ [Perspective Monde \(2020\)](#). We use real data given in Fig. 12 and the *EnKf* procedure for the reconstruction of both the state variables and unknown transmission rates of COVID-19 in Gabon. The results of numerical simulations are depicted in Figs 13–16.

Figure 13 provides the estimation of the parameters which influenced the transmission rates in Gabon. It is β_{d0} , β_u , β_{v0} , r_d , r_u and r_v . Figure 14 presents the estimations of parameters p , q , ω , δ , d_d and θ while the reconstruction of the transmission rates β_d , β_u and β_v are depicted in Fig. 15. After the lockdown, the contact rates and efficacies of controls remain almost constant in Gabon (see the magenta lines in Fig. 13(a)–(f)). So the transmission rates remain constant during the same period (see the magenta lines in Fig. 15(a)–(c)). However, except the transmission rate β_u that decreased, the other ones remained constant during the lockdown in Gabon (see the blue lines in Figs 13(a)–(c) and 15(a)–(c)). The results show that after a relaxation of the preventive measures, Gabonese continuous to practice distancing measures with detected cases more than undetected ones and the practice of distancing measures with the free SARS-CoV-2 in the environment has significantly increase (see the red lines

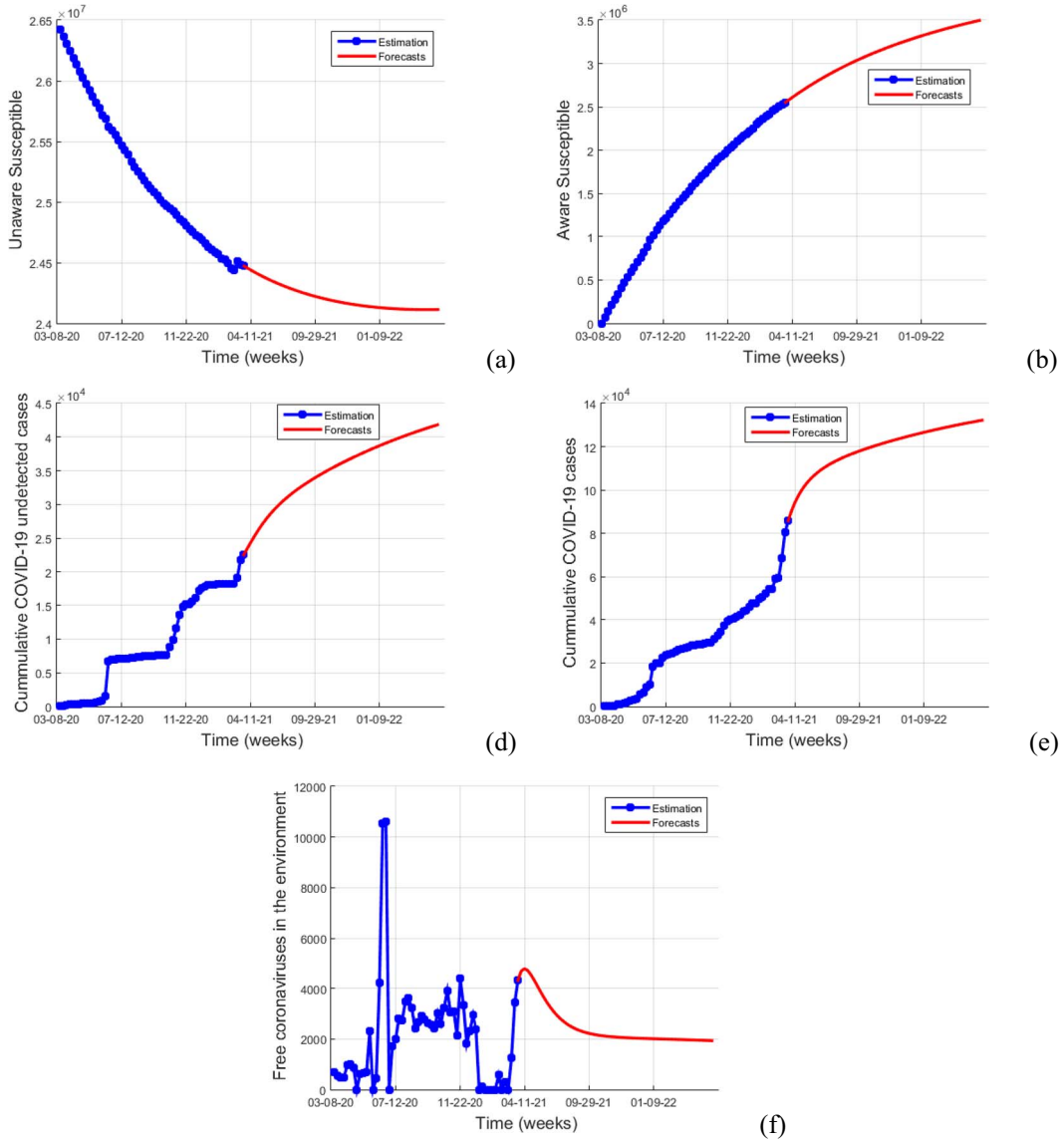


FIG. 11. Short term forecasting of COVID-19 pandemic in Cameroon of: (a) unaware susceptible individuals S_u ; (b) aware susceptible individuals S_a ; (d) cumulative COVID-19 undetected cases; (e) cumulative COVID-19 cases and (f) free SARS-CoV-2 viruses in the environment V .

in Fig. 13(d)–(f)). In summary, we find that after relaxing the preventive measures, the transmission rate β_u increased (see the red lines in Fig. 15(b)) in contract with the transmission rates β_d and β_v , which increased and decreased at some time (see the red line in Fig. 15(b) and (c)). The results in Fig. 14 show that during the first nine weeks, the detection rate ω has not varied enough in Gabon. The same results are observed for the proportions p , q and δ , which are around 9.5%, 43.2% and 11.8%, respectively (see

TABLE 6 Forecasts of COVID-19 cases in Cameroon on July 10, 2022.

States	Detected cases		Undetected cases		Total cases	
	Active	Cumulative	Active	Cumulative	Active	Cumulative
Values	26	28288	46	33 118	72	61 406

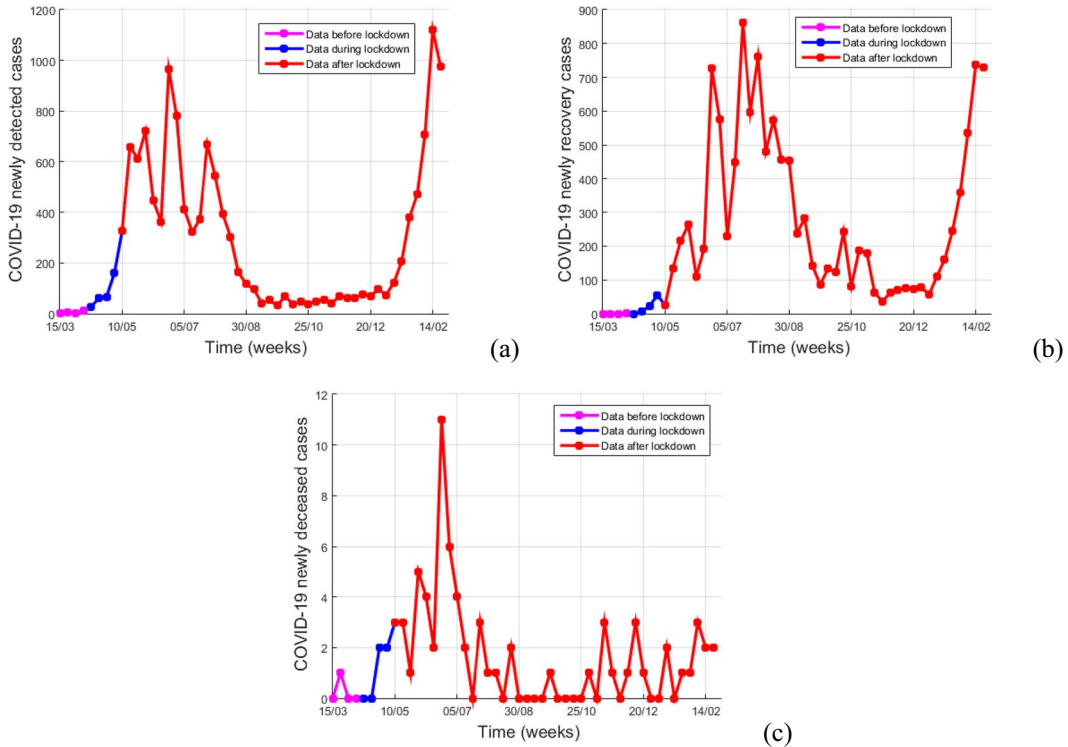


FIG. 12. Reported data of COVID-19 from 12-03-2020 to 21-02-2021 in Gabon (Politologue.com, 2020). (a) New cases, (b) newly recovered individuals and (c) newly deceased.

the magenta lines in Fig. 14(c)–(f). However, we note that the majority of new infected unaware is not directly detected in Gabon (more than 70% are not detected immediately, see Fig. 14(d)). And, 44% the new infected aware are directly detected after lockdown (see Fig. 14(e)), which correlate with the fact that aware individuals are more conscious than unaware ones about the existence of COVID-19 in Gabon. Even if these proportions did not vary enough, we globally point out a sharp increase of q during the estimation periods (see the red lines in Fig. 14(e)), a strongly decrease of p after relaxing measures. Also, the detection rate of the undetected cases $\delta\omega$ has been increased significantly after relax measures (see the red line in Fig. 14(c) and (f)).

Reset, we estimate the state variables of system (4) during the three estimation periods to fit the COVID-19 data in Gabon. Figure 17 gives the results. We find that the estimated state variables of system (4) with the Gabonese parameters fit the data of COVID-19. In fact, the estimated values are very good, since the trajectories of estimated cases (green lines) follow better the data values (in star

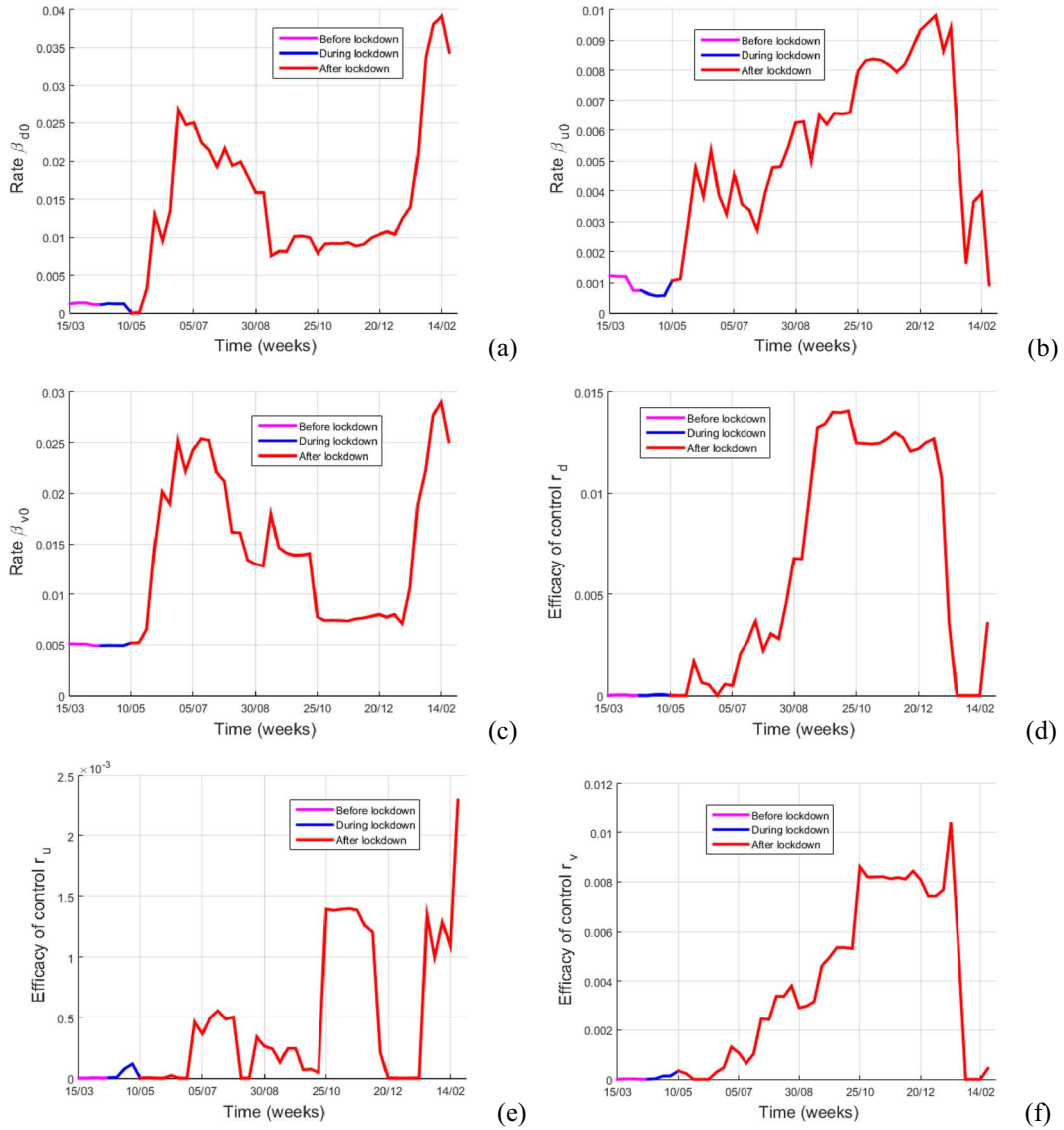


FIG. 13. Estimation of the transmission rates in Gabon from March 15, 2020, to February 21, 2021. (a) Transmission rate from detected cases without interventions $\beta_{d,0}$. (b) Transmission rate from undetected cases without interventions $\beta_{u,0}$. (c) Transmission rate from free SARS-CoV-2 in the environment without intervention $\beta_{v,0}$. (d) Decay rate of human contacts with detected cases r_d . (e) Decay rate of human contacts with undetected cases r_u . (f) Decay rate of human contacts with free SARS-CoV-2 in the environment r_v .

cloud) as shown in Fig. 17(a)–(e). Then, one can use these estimated states to reconstruct the COVID-19 undetected cases since the beginning of the pandemic in Gabon. And to do this, we use the estimated values of states and parameters of system (4) to reconstruct the weekly undetected cases and the total cases in Gabon.

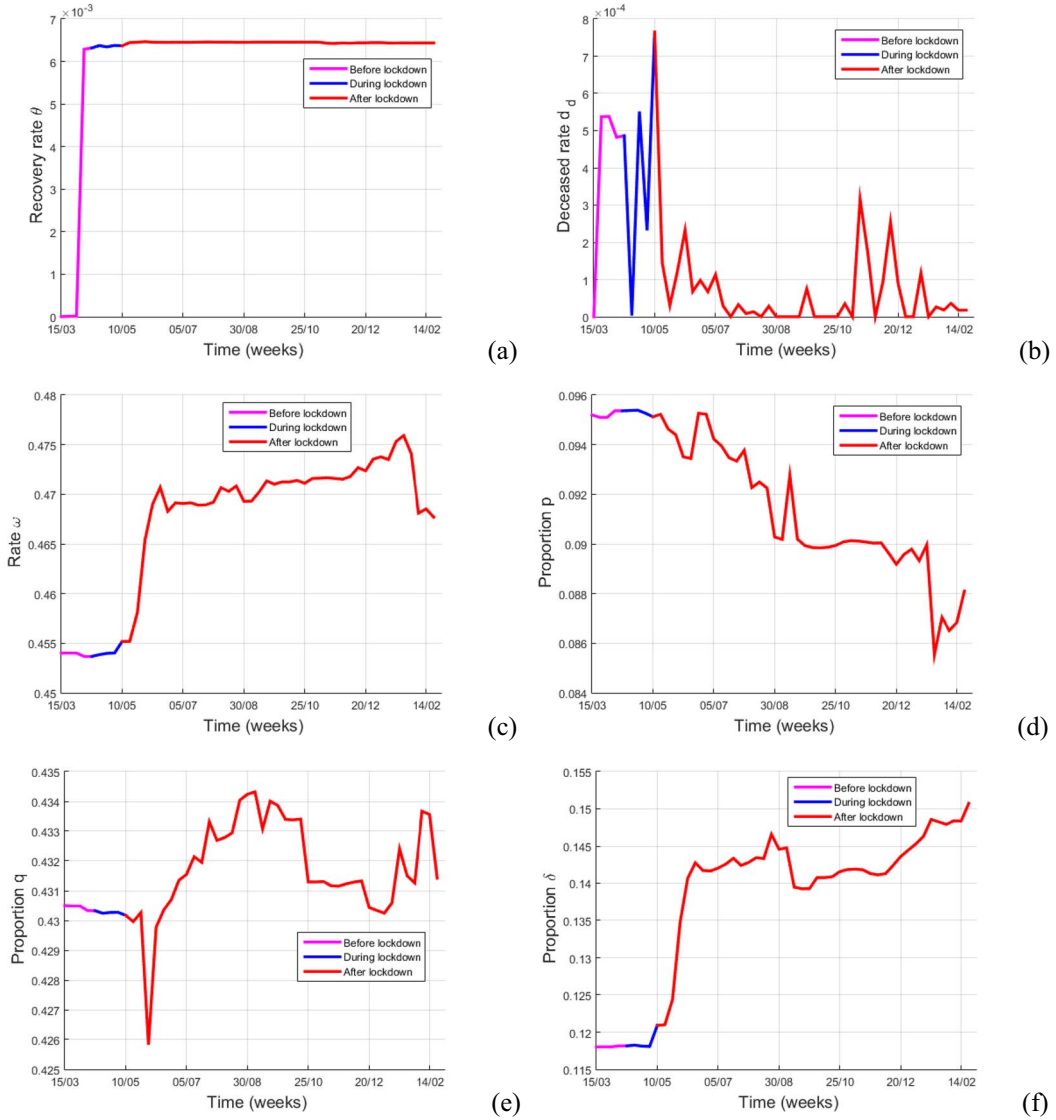


FIG. 14. Estimation of unknown parameters of COVID-19 pandemic in Gabon using the initial conditions $(2183590, 0, 1, 5, 0, 700)$ and the initial parameters $(0.00123, 0.00123, 0.0051, 0, 0, 0, 0, 0.0952, 0.4305, 0.454, 0.118)$. (a) Recovery rate θ ; (b) deceased rate d_d ; (c) screening rate ω ; (d) proportion p ; (e) proportion q and (f) proportion δ .

Figure 18 shows the results. Figure 8(a) gives the evolution of the number of newly undetected cases, and Fig. 18(b) and (c) the number of active undetected cases and cumulative undetected cases, respectively, who remained unknown by the health authorities. It turns out that, even if some of these individuals are either detected or recovered (see Fig. 18(b)), others continue to transmit COVID-19 within the Gabonese population. Also, we fit the total cases in Gabon by adding the detected and undetected cases from March 15 to February 21, 2021. The results are plotted in Fig. 18(d)–(f). To

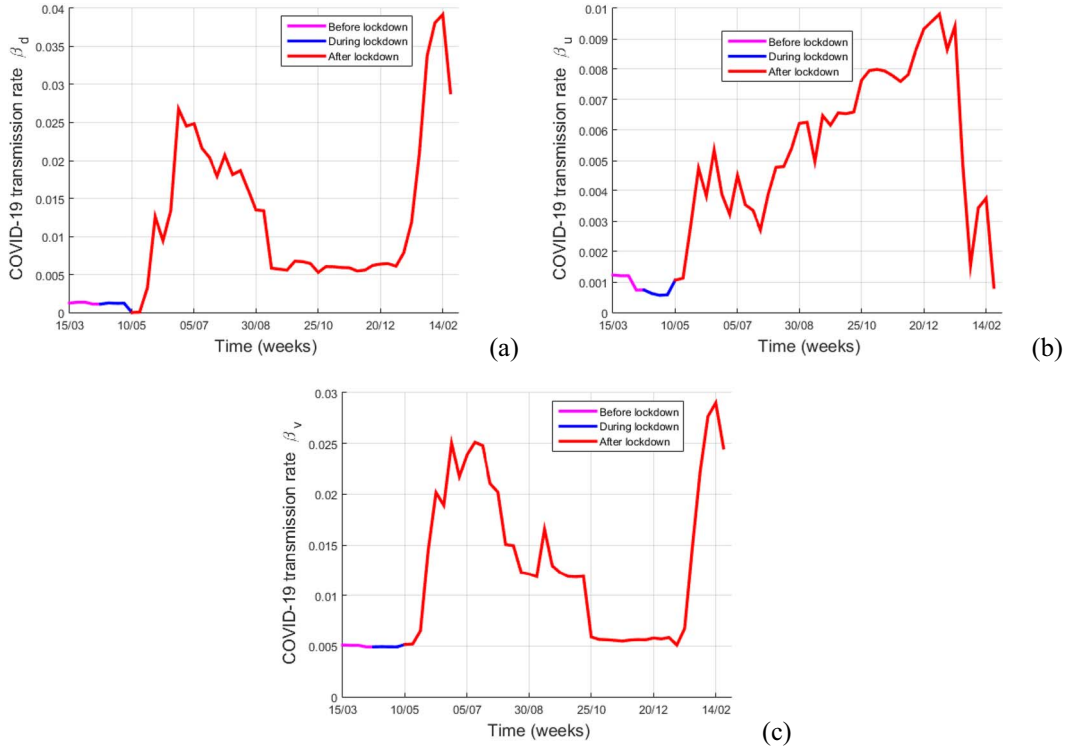


FIG. 15. Estimation of transmission rates in Gabon since the beginning of COVID-19 until on April 04, 2021, using the estimated values of unknown parameters. (a) Transmission rate from detected cases β_d , (b) transmission rate from undetected cases β_u and (c) transmission rate from free SARS-CoV-2 in the environment β_v .

add further evidence of these results, we fit the basic reproduction number since the beginning of the COVID-19 in Gabon using the estimated values of parameters. The results are plotted in Fig. 15(f). All the above curves imply that after the relaxation of the control measures, the pandemic continues to increase before started to decrease as shown each red line of total cases on Fig. 8(d)–(f). It is observed that during the same period, the concentration of free SARS-CoV-2 in the environment significantly decreases after a first increase (see Fig. 16(f)). Also, we present the summary of the situation of COVID-19 cases in Gabon at the date of February 21, 2021 in Table 7. We give the mean values of estimated parameters of system (4) in Table 8. With this on mind, the estimated mean value of the basic reproduction number during the estimation period is $\mathcal{R}_0 \approx 1.0379$. So the COVID-19 pandemic will not die out ($\mathcal{R}_0 > 1$) without any control measures in Gabon as in Cameroon that aim at bringing this basic reproduction number below one.

3.5.2 Forecast of COVID-19 pandemic in Gabon. Here, we use the above results to make a short-term prediction of the evolution of the COVID-19 pandemic in Gabon after one year. For this, we take the initial conditions for system (4) at February 21, 2021, the current estimated states given in Table 9. Now, the unknown parameters for system (4) are known and their values are reported after the estimation of Gabon cases in Table 8. We use these parameters values to give the COVID-19 trend in Gabon. We

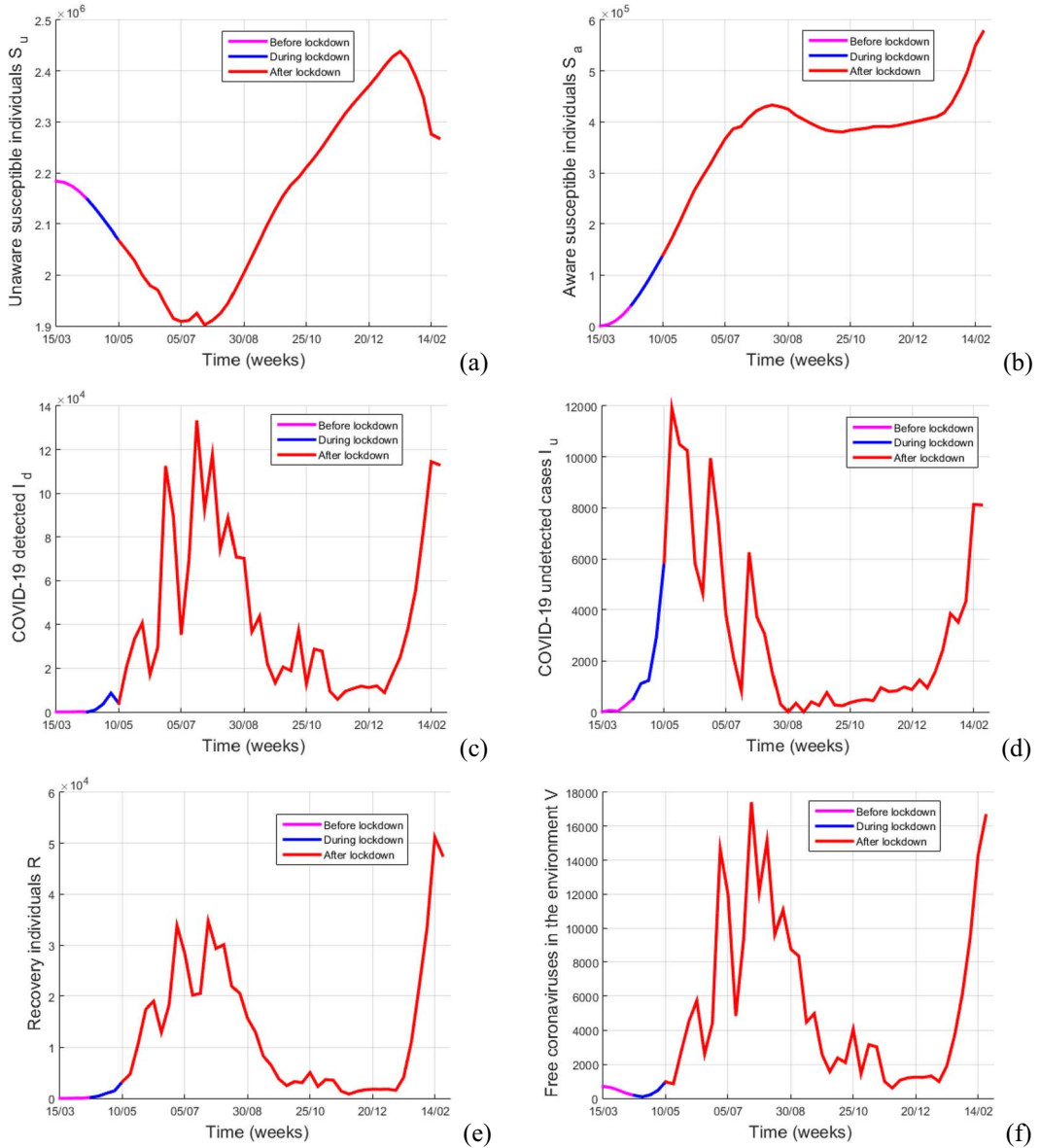


FIG. 16. Estimation of unmeasurable states of COVID-19 pandemic in Gabon using the initial condition $(2183590, 0, 1, 5, 0, 700)$ and the initial parameters $(0.00123, 0.00123, 0.0051, 0, 0, 0, 0, 0.0952, 0.4305, 0.454, 0.118)$. (a) Unaware susceptible individuals S_u ; (b) aware susceptible individuals S_c , (c) detected cases I_d , (d) undetected cases I_u , (e) recovered individuals R and (f) free SARS-CoV-2 in the environment V .

did the forecasts for the period going to February 21, 2021 to April 09, 2022. As in Cameroon, we compare the real data from February 21 to April 25, 2021, with the first prediction estimated with the EnKf without using these data. The results are plotted in Fig. 19. Figure 20 presents the forecast of the

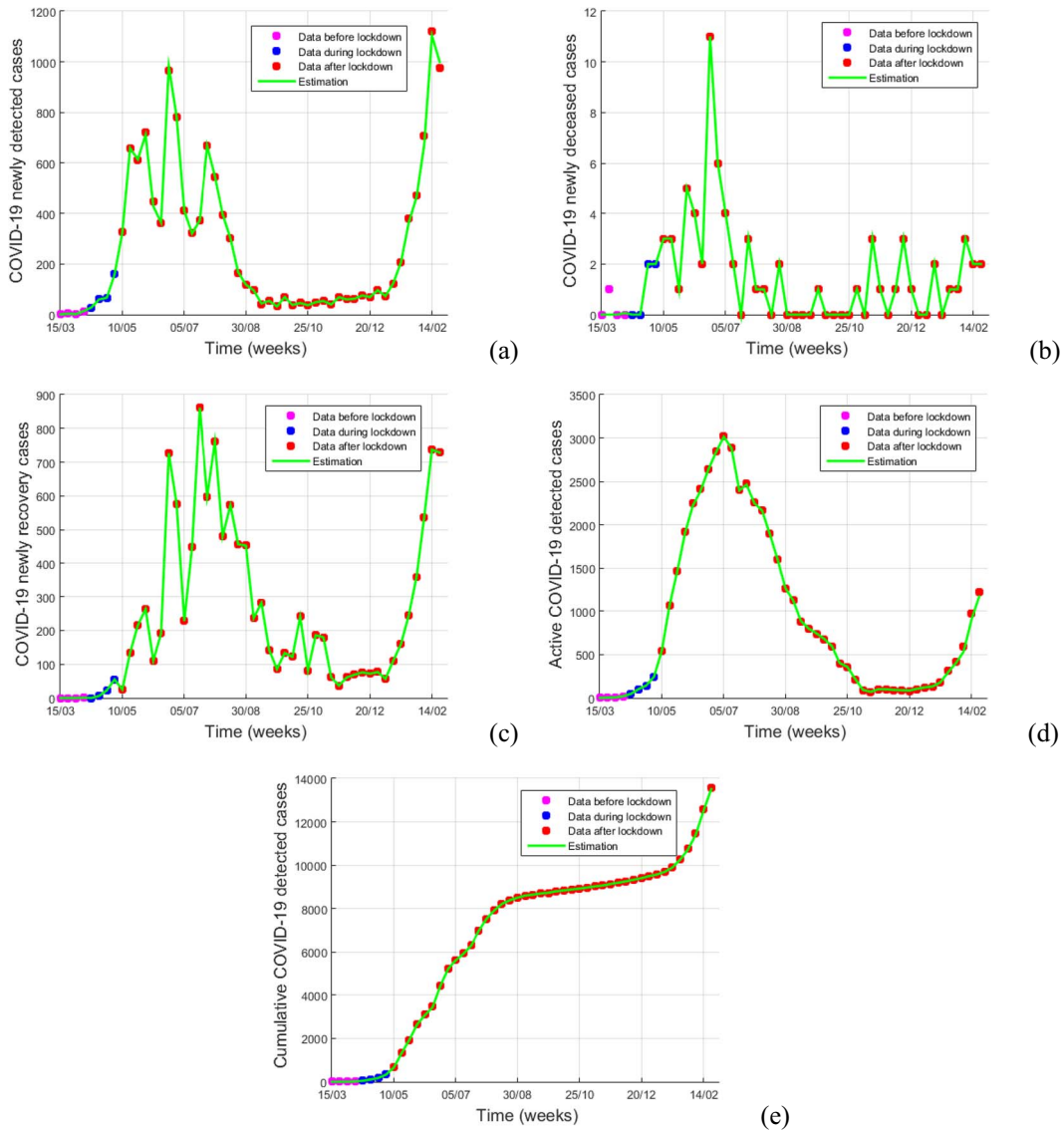


FIG. 17. Fitting results of the current COVID-19 pandemic in Gabon using the estimated values of the transmission rates β_d and β_v given in Fig. 14. (a) Newly reported cases, (b) newly deceased cases, (c) newly recovery cases, (d) active detected cases and (e) cumulative detected cases.

undetected and the newly and active cases in Gabon. Without efforts in this country, the second pandemic may be more serious than the previous one as shown in the forecasts of the active cases (see blue, red and green lines in Fig. 19(d) and Fig. 20(b) and (d)). However, the process of screening for active undetected cases will bear more fruit from the twenty-eighth week. Indeed, the detected individuals will gradually increase as undetected individuals (see the red lines in Fig. 19(c) and Fig. 20(a) and (c)).

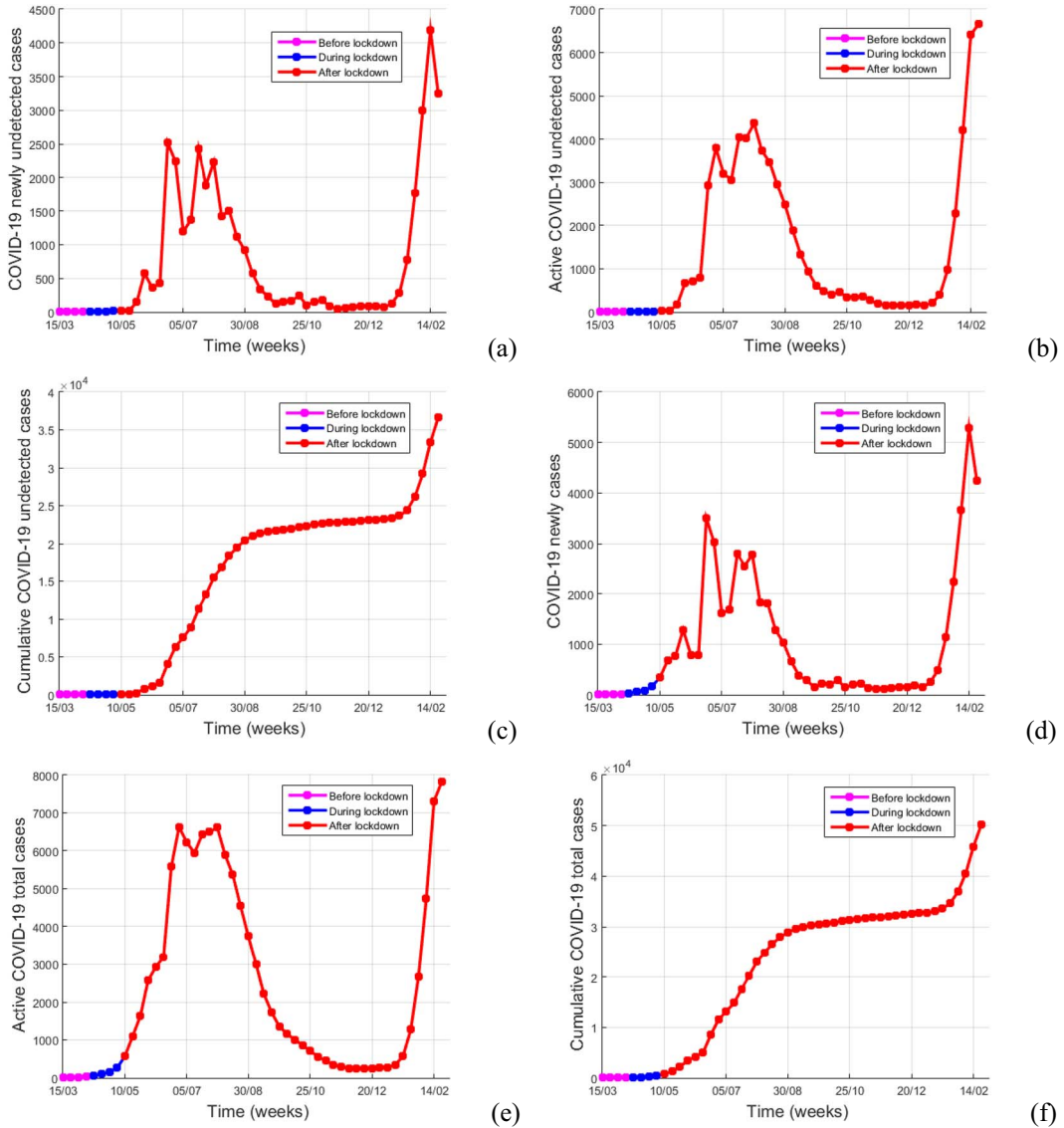


FIG. 18. Reconstruction of COVID-19 undetected cases in Gabon using the estimated values of both states and parameters of system (4) given in fig 3- 6. (a) Newly undetected cases; (b) active undetected cases; (c) cumulate undetected cases; (d) total newly cases; (e) total active cases and (f) total cumulative cases.

Thus, accelerating the healing process will put an end to this pandemic in Gabon since many would not die from this disease but will cure (see Fig. 19(b) and (c)). The forecasts show that the concentration of free SARS-CoV-2 in the environment will continue to increase (see the red lines in Fig. 21(f)) and that the aware and unaware individuals will increase (see the red lines in Fig. 21(a) and (b)). We report the expected trend of COVID-19 in Gabon at the date of April 09, 2022, on Table 10.

TABLE 7 States of COVID-19 in Gabon on February 21, 2021.

Variables	Detected cases		Undetected cases		Total cases	
	Active	Cumulative	Active	Cumulative	Active	Cumulative
Values	1216	13 553	6 655	36 617	7 824	50 122

TABLE 8 Mean values of estimated parameters of the COVID-19 in Gabon on February 21, 2021.

Parameters	Values	Parameters	Values
β_{d0}	0.03443	β_{u0}	0.00092
β_{v0}	0.02509	r_d	0.00355
r_u	0.00229	r_v	0.00044
d_d	0.00001	θ	0.00643
p	0.08809	q	0.43142
ω	0.46770	δ	0.15073
β_d	0.02892	β_u	0.00082
β_v	0.02455	\mathcal{R}_0	1.0379

TABLE 9 Estimated values of state variables of system (4) in Gabon on February 21, 2021.

Variables	S_u	S_a	I_d	I_u	R	V
Values	2 267 969	576 991	113 097	81 118	476 409	166 271

4. Discussions and conclusion

In this paper, we have described and illustrated a method to estimate unmeasured state variables and unknown parameters (that are assumed to be time-dependent for transmission rates and constant for other ones) in a COVID-19 mathematical model using real data. We have first proposed a mathematical model for the dynamical transmission of COVID-19 within a human community of sub-Saharan Africa that takes into account: (i) the compliance of preventive methods against COVID-19 through awareness programs; (ii) the stigmatization and ignorance of some COVID-19 patients that are not present to the authorities in charge of the disease for a screening after the appearance of first symptoms and (iii) non-pharmaceutical interventions such as mass media-based sensitization, social distancing, face-mask wearing, contact tracing and the disinfection and decontamination of infected places by using suitable products against free SARS-CoV-2 in the environment in order to reduce the spread of the disease. Also, we assumed that the transmission rates are influenced from time to time by distancing measures as recommended by WHO to reduce contacts between either human and human or human and the free SARS-CoV-2 in the environment during the COVID-19 period. We have studied the basic properties of the model, such as the positivity of solutions and the boundedness of the trajectories of the considered model. Assuming constant parameter values, we also have computed the disease-free equilibrium and derived the basic reproduction number that determines the outcome of COVID-19. We used the EnKf approach to reconstruct the unmeasurable state variables and unknown parameters of the formulated COVID-19 dynamics model using real data. This model has been calibrated using the current COVID-19 pandemic firstly from March 08, 2020, to April 04, 2021, in Cameroon and secondly from March 15, 2020, to February 21, 2021, in Gabon.

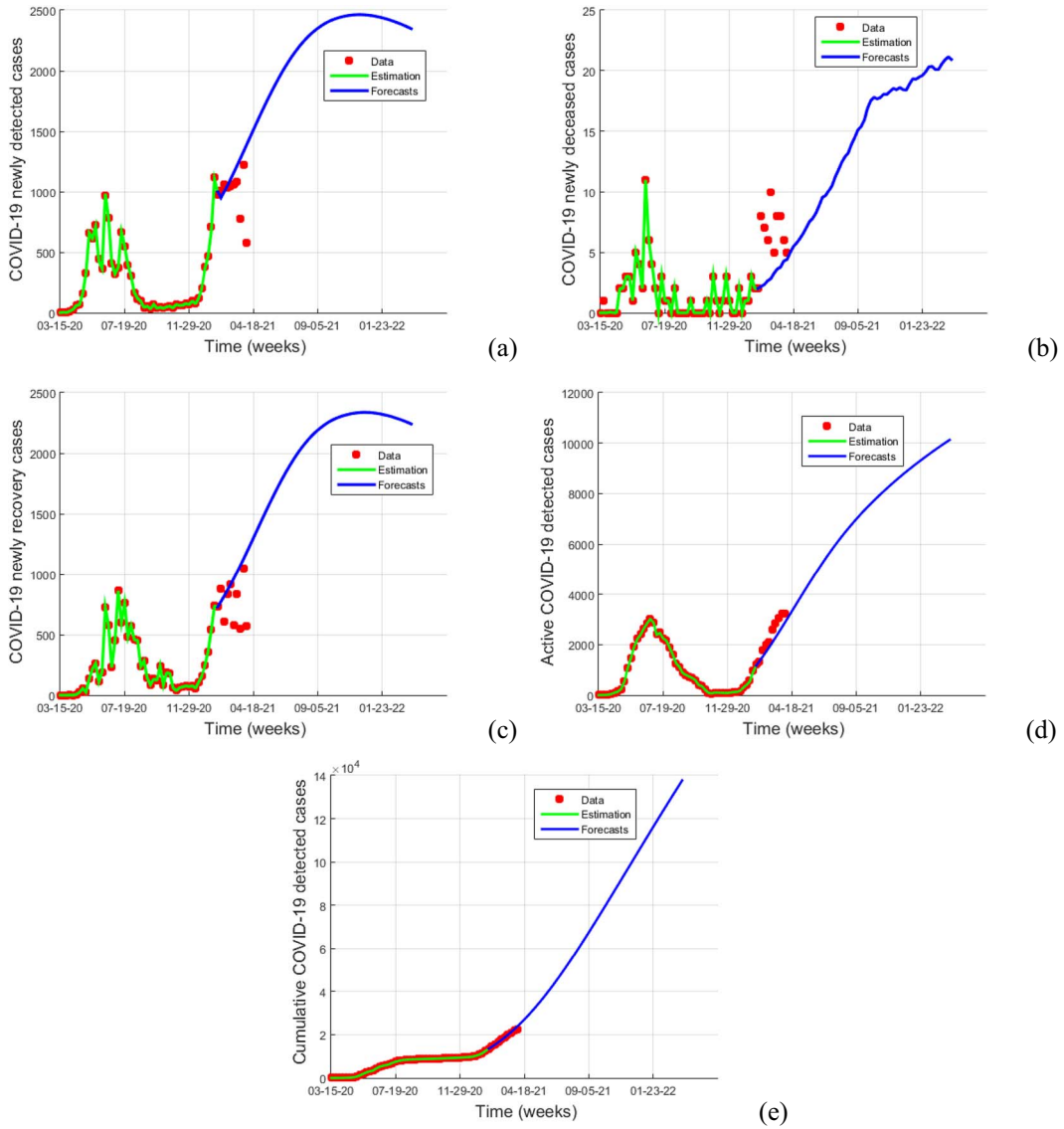


FIG. 19. Short-term forecasting of newly and active cases of COVID-19 pandemic in Gabon. (a) COVID-19 newly detected cases; (b) COVID-19 newly deceased; (c) COVID-19 newly recovered COVID-19 cases; (d) active COVID-19 detected cases; and (e) cumulative COVID-19 detected cases.

Our main results on the estimation of the COVID-19 pandemic in Cameroon can be summarized as follows. (i) The estimation of the state variables and unknown parameters fit the data well. (ii) The distancing measures remain low, since the estimated values of r_d , r_u and r_v are small compared to unity. Also, more than 35% of aware susceptible who contract the COVID-19 are directly detected and also less than 7% of unaware susceptible are directly detected. This suggests that the majority of COVID-19

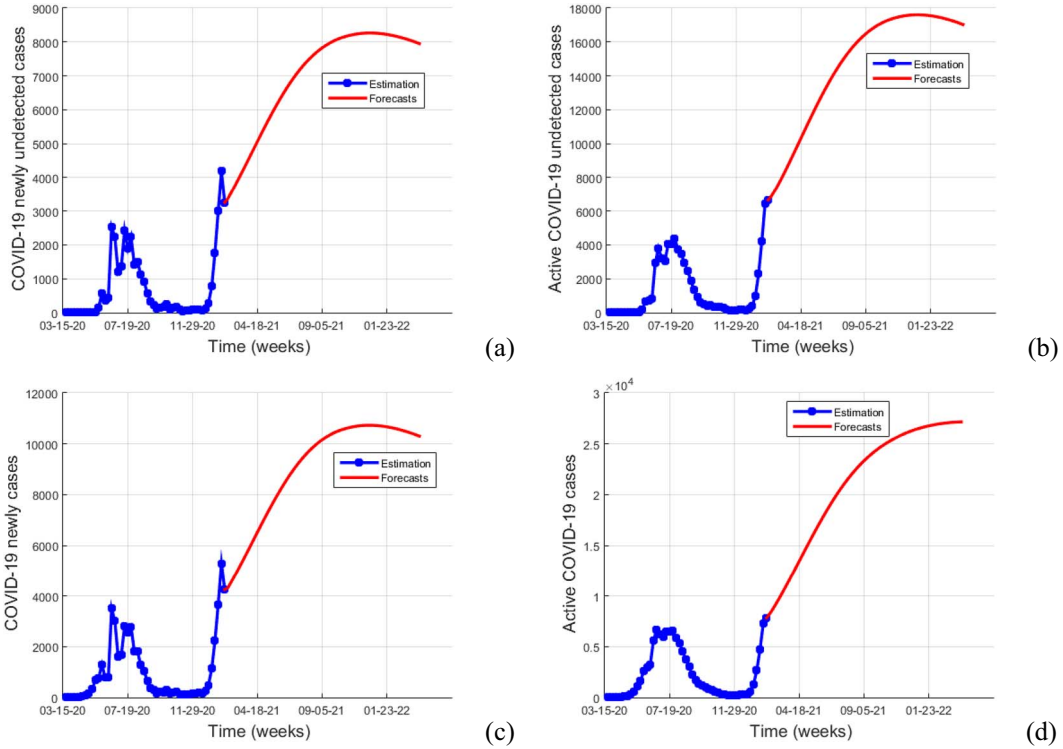


FIG. 20. Short-term forecasting of newly and active cases of COVID-19 pandemic in Gabon. (a) COVID-19 newly undetected cases; (b) active COVID-19 undetected cases; (c) COVID-19 new cases and (d) active COVID-19 cases.

cases fear the stigmatization and prefer to stay home for self-treatment. However, it is absurd that many people including those who are aware about COVID-19 prefer to hide themselves. This result is in line with the statement of WHO that many individuals who have or suspected to suffer from COVID-19 and those who recovered are stigmatized in their community (UNICEF, 2020c). (iii) The number of active undetected cases is high and represents approximately the half of the detected cases. This can be explained by the irregular reporting of infectious cases, since the cases appear after two or four days without any new cases. According to these results, there will have already been more than 5150 active cases not diagnosed by Cameroonian healthcare staff in the evening of April 04, 2021. However, the proportion of detection rates δ of these cases remains high given the ratio between the number of detected and undetected cases. Thus, these undetected cases will be detected at time if healthcare keeps up the speed of awareness campaign. Also, at this date Cameroon could have more than 31 000 active cases of versus 87 250 cases in total. (iv) The concentration of the free SARS-CoV-2 in the environment has firstly increased, but has decreased even if it still persists. (v) The number of infected cases (detected or not) can decrease if the Cameroonian government continuous to apply preventive measures from the free SARS-CoV-2 in the environment, as the mean value of the basic reproduction number at the date of April 04, 2021, among the human individuals is clearly less than the unity (i.e. $\mathcal{R}_{0h} = 0.05$). We stress that five parameters have not been estimated and have been selected hypothetically based on the results of the sensitivity analysis of the model and numerical tests. Indeed, the EnKf approach

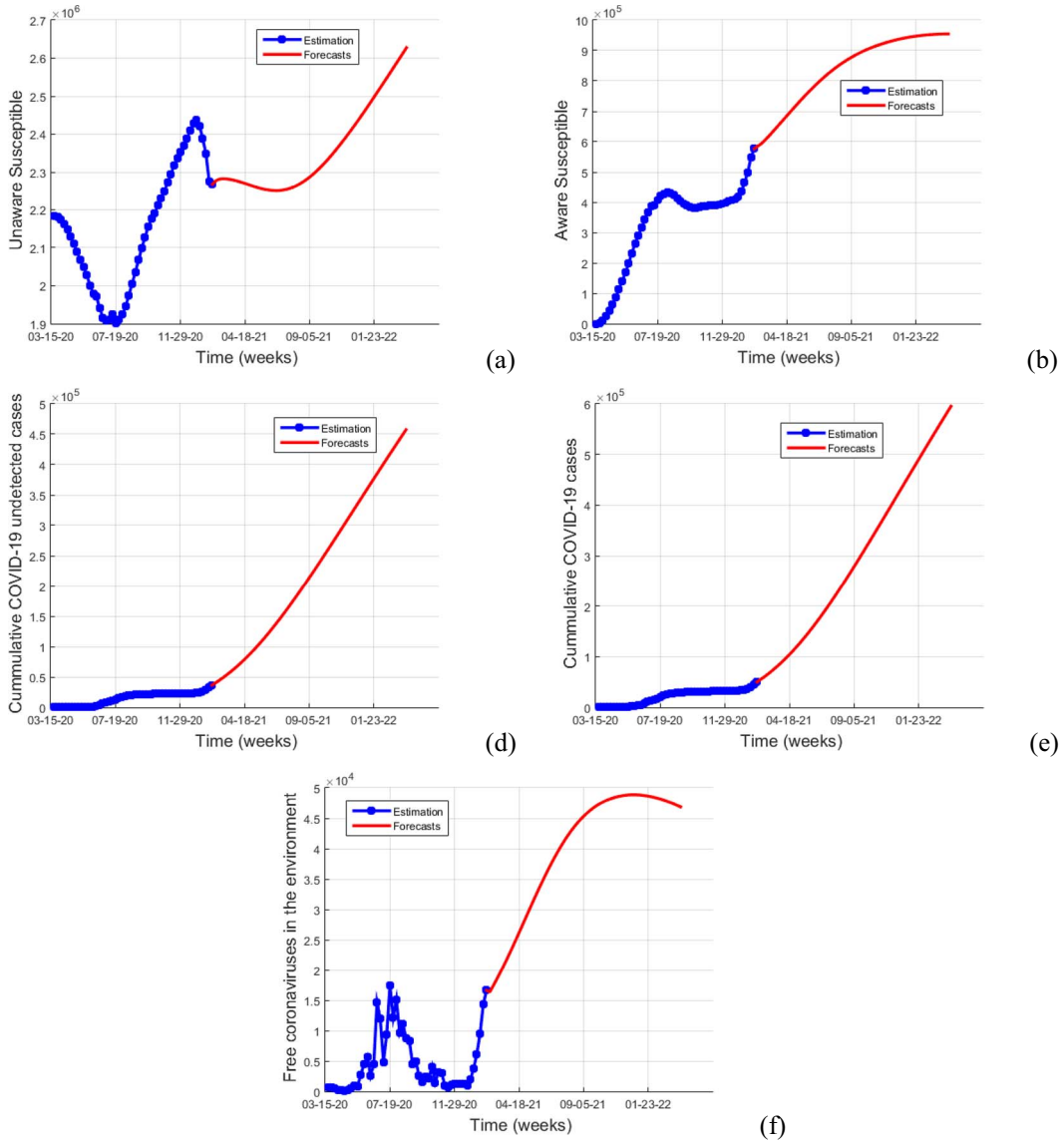


FIG. 21. Short-term forecasting of COVID-19 pandemic in Gabon of (a) unaware susceptible individuals S_U ; (b) aware susceptible individuals S_A ; (d) cumulative COVID-19 undetected cases; (e) cumulative COVID-19 cases and (f) free SARS-CoV-2 viruses in the environment V .

has the advantage to self-correct unmeasurable variables and unknown parameters during the fitting of observed data.

We summarize the main results on the COVID-19 pandemic in Gabon as follows. (a) The estimation of the state variables and unknown parameters fit the data of Gabon well. (b) The distancing measures around human individual do not head to better results like those implemented in Cameroon. (c) The

TABLE 10 *Forecasts of COVID-19 cases in Gabon at April 09, 2022.*

Variables	Detected cases		Undetected cases		Total cases	
	Active	Cumulative	Active	Cumulative	Active	Cumulative
Values	10 127	137 670	17 028	457 340	27 155	595 020

TABLE 11 *Performance of prevision.*

Performance Metrics	Country	COVID-19 newly Reported cases	COVID-19 newly Deceased cases	COVID-19 newly Recovered individuals
MAE	Cameroon	1 045	95	0
	Gabon	206	3	237
RMSE	Cameroon	1 470	105	0
	Gabon	328	4	316

undetected cases was high within the population during and after the first vague. This can be explained by the delay in the report of infectious cases. According to these results, there will have already been more than 6500 active cases not diagnosed by Gabonese healthcare staff compared to 1250 diagnosed on the date of February 21, 2021. Moreover, the detection rate of these cases increases time to time. This confirms why the detected cases are very less compared to the undetected cases. (d) The concentration of the free SARS-CoV-2 in the environment persists but have significantly decreased after the first vague but, started to grow afterwards. (e) The number of COVID-19 cases (either detected or undetected) will quickly increase if nothing is done to reduce the transmission rates (which have a high average value) since the estimated value of basic reproduction number at the date on February 21, 2021, is clearly larger than unity (i.e. $\mathcal{R}_0 = 1.43 > 1$) in Gabon. (f) Unlike Cameroon, unaware individuals in Gabon take more precautions since more than 8% are directly detected after the contagion. Thus, as part of the fight against this pandemic, we could focus on awareness campaigns as merely 43.8% of aware individuals are directly detected.

A comparative study during the estimation period shows that the transmissions from the free SARS-CoV-2 in the environment is greater than that from the infected individuals in Cameroon with $\mathcal{R}_{0h} = 0.05721$ and $\mathcal{R}_{0v} = 1.78051$. This imply that Cameroonians apply distancing measures between individual more than with the free SARS-CoV-2 in the environment. But, the opposite is observed in Gabon with $\mathcal{R}_{0h} = 0.63899$ and $\mathcal{R}_{0v} = 0.39894$. So, it is important to increase the awareness campaigns to reduce contact from individual to individual in Gabon.

The performance metrics of the forecasts are reported in Table 11. From Table 11, it is evident that the model can perfectly give the short-term forecasts situation of COVID-19 both in Cameroon and Gabon.

In summary, the number of undetected cases remains high in both countries, which would undoubtedly be at the origin of this second wave of the COVID-19 pandemic. In fact, any government can declare the COVID-19 pandemic over when the number of detected cases is zero. Unfortunately, the undetected cases will continue to rise in the population and either trigger or increase a new epidemic. This was observed in the Spanish flu. Also, we can understand that COVID-19 does not always make too many victims in Cameroon and Gabon perhaps because of the traditional pharmacopoeia much appreciated locally or because of the fact that several of these undetected cases are asymptomatic and either recover or die quickly. A comparative study shows that there are more undetected cases in

Cameroon than in Gabon, maybe because of the greater size of the Cameroonian population compared to Gabon. The opposite has been observed in the detected cases. In Gabon, between the end of the first wave and the start of the current wave, susceptible individuals were not continuously aware as in Cameroon. This could also justify the high incidence of COVID-19 at the start of this second wave. Also, a comparison between the basic reproduction number from human individuals \mathcal{R}_{0h} and from the SARS-CoV-2 in the environment \mathcal{R}_{0v} has been done in Cameroon and Gabon. The results can answer to the question that: why the lockdown was not the solution to cope with the pandemic in Cameroon but, was the solution to cope with it in Gabon. In contrast, the disinfection and decontamination of infected places and strict compliance to hygiene rules are a solution to cope the COVID-19 pandemic in Cameroon. Also, this implies that this COVID-19 pandemic is spreading randomly from country to country. To cope with the current COVID-19 pandemic, the first control measures in Cameroon should be to turn on several measures lifted and secondly, to implement total or partial lockdown in Cameroon as recommended WHO. It is then important to apply control measures such as contact tracing, social distancing, face-mask wearing, isolation of patient, pharmaceutical interventions and the disinfection and decontamination of infected places by using suitable products against free SARS-CoV-2 in the environment. However, the results of this work make it possible to accept the relaxation of the distancing measures but this must be followed by a massive sensitization of the population reinforced by large-scale testing in order to detect cases which continue to transmit COVID-19 without being aware of this. A question remains open, however, that concerning the estimation of the lost to follow-up, i.e. those who are screened but their status remains unknown thereafter. Such work could explain why we have not observed cured cases since March 14, 2021, in Cameroon or on certain days in both countries.

REFERENCES

- ADHIKARI, S. P., MENG, S., WU, Y-J., MAO, Y-P., YE, R-X., WANG, Q-Z., SUN, C., SYLVIA, S., ROZELLE, S., RAAT, H. & ZHOU, H. (2020) Epidemiology, causes, clinical manifestation and diagnosis, prevention and control of coronavirus disease (COVID-19) during the early outbreak period: a scoping review. *ADHIKARI et al. Infect. Dis. Poverty*, **1**, 9–29.
- BARBAROSSA, M. V., FUHRMANN, J., MEINKE, J. H., KRIEG, S., VARMA, H. V., CASTELLETTI, N. & LIPPERT, T. (2020) Modeling the spread of COVID-19 in Germany: early assessment and possible scenarios. *PLoS One* **15**, e0238559. <https://doi.org/10.1371/journal.pone.0238559>
- BOURGOIS, L., ROUSSEL, G. & BENJELLOUN, M. (2011) Kalman d'ensemble état-paramètres appliqué au modèle de Lorenz. <https://www-lisic.univ-littoral.fr/publis/1323537933.pdf>. August 05, 2019.
- BOWONG, S. & KURTHS, J. (2010) Modelling tuberculosis and hepatitis B co-infections. *Math. Model. Nat. Phenom.*, **5**, 196–242.
- BRAS, R. L. & RODRIGUEZ-ITURBE, I. (1994) *Random Functions and Hydrology*. Dover Publications.
- Business Today (2021) *In 20-30% recovered people lose natural immunity against COVID-19 in 6 months.* <https://www.businesstoday.in/latest/trends/story/20-30-recovered-people-lose-natural-immunity-against-covid-19-in-6-months-293192-2021-04-11>. July 01, 2021. Visited on April 11, 2021.
- CHAN, J. W. M., NG, C. K., CHAN, Y. H., et al. (2003) Short term outcome and risk factors for adverse clinical outcomes in adults with severe acute respiratory syndrome (SARS). *Thorax*, **58**, 686–689.
- CHAO, D. L., LONGINI, I. M. & MORRIS, J. G. (2014) Modeling cholera outbreaks. *Curr. Top. Microbiol. Immunol.*, **379**, 195–209.
- CHEN, N., ZHOU, M., DONG, X., et al. (2020) Epidemiological and clinical characteristics of 99 cases of 2019 novel coronavirus pneumonia in Wuhan, China: a descriptive study. *Lancet*, **395**, 507–513.
- CHOWDHURY, R., HENG, K., SHAWON, M. S. R., GOH, G., OKONOFUA, D., ROSALES, C. O., JARAMILLO, V. G., BHUIYA, A., REIDPATH, D., PRATHAPAN, S., SHAHZAD, S., ALTHAUS, C. L., JARAMILLO, N. G. & FRANCO, O.

- H. (2020) Dynamic interventions to control COVID-19 pandemic: a multivariate prediction modelling study comparing 16 worldwide countries. *Eur. J. Epidemiol.* **35**, 389–399.
- COVID-19 pandemic in Cameroon (2020) https://en.wikipedia.org/wiki/COVID-19_pandemic_in_Cameroon. May 01, 2020.
- DANIELLE RENWICK (2020) How long does coronavirus live on different surfaces? <https://www.theguardian.com/us-news/2020/apr/04/how-long-does-coronavirus-live-on-different-surfaces>. May 04, 2020.
- EIKENBERRY, S. E., MANCUSO, M., IBOI, E., PHAN, T., EIKENBERRY, K., KUANG, Y., KOSTELICH, E. & GUMEL, A. B. (2020) *To Mask or Not to Mask: Modeling the Potential for Face Mask Use by the General Public to Curtail the COVID-19 Pandemic*. Tempe, AZ, USA, April 8: Arizona State University, School of Mathematical and Statistical Sciences.
- EKONDE, D. (2020) The challenge with African countries promoting traditional cures for Covid-19 without research. <https://qz.com/africa/1852069/african-countries-want-to-boost-traditional-cures-for-covid-19/>, QUARTZ AFRICA. Updated on May 6, 2020.
- FEI, Z., TING, Y., RONGHUI, D., GUOHUI, F., YING, L., ZHIBO, L., JIE, X., YEMING, W., SONG, B., GU, X., GUAN, L., WEI, Y., LI, H., WU, X., XU, J., TU, S., ZHANG, Y., CHEN, H. & CAO, B. (2020) Clinical course and risk factors for mortality of adult inpatients with COVID-19 in Wuhan, China: a retrospective cohort study. March 12, 2020.
- FOUOGUE, J. T., NOUBOM, M., KENFACK, B., DONGMO, N. T., TABEU, M., MEGOZEU, L., ALIM, J. M., FOGANG, Y. F., RIM, L. C. N., FOUELIFACK, F. Y., FOUEDJIO, J. H., MANEBOU, P. L. F. N., BIBOU ZE, C. D., KOUAM, B. F., FOMETE, L. N., TEBEU, P. M., KEMFANG, J. D. N., FOUMANE, P., SANDO, Z. & OROCK, G. E. E. (2020) Poor knowledge of COVID-19 and unfavourable perception of the response to the pandemic by healthcare workers at the Bafoussam Regional Hospital (West Region-Cameroon). *Pan African Med. J.*, **37**, 19. <http://10.11604/pamj.sup.2020.37.1.25688>.
- FUNG, I. C.-H. (2014) Cholera transmission dynamic models for public health practitioners. *Emerg. Themes Epidemiol.*, **1**, 1–11.
- Gabonactu.com (2020) Gabon records its first cured case of Covid-19. Update on April 2nd and visited on July 26, 2020. <https://gabonactu.com/le-gabon-enregistre-son-premier-cas-gueri-du-covid-19/>
- GATTO, M., BERTUZZO, E., MARIA, L., MICCOLI, S., CARRARO, L., CASAGRANDE, R. & RINALDO, A. (2020) Spread and dynamics of the COVID-19 epidemic in Italy: effects of emergency containment measures. *Proc. Natl. Acad. Sci.*, **117**, 10484–10491. DOI: <https://doi.org/10.1073/pnas.2004978117>
- GHOSH, I. & MARTCHEVA, M. (2021) Modeling the effects of prosocial awareness on COVID-19 dynamics: case studies on Colombia and India. *Nonlinear Dynam.*, **104**, 4681–4700. <https://doi.org/10.1007/s11071-021-06489-x>
- GICAM worried about impacts of Coronavirus on Cameroon's economy (2020) <https://www.businessincameroon.com/economy/1103-10070-gicam-worried-about-impacts-of-coronavirus-on-cameroon-s-economy>. Visited on May 13, 2020.
- GILLJNS, S., BARRERO MENDOZA, O., CHANDRASEKAR, J. DE MOOR, B. L. R., BERNSTEIN, D. S. & RIDLEY, A. (2006) What is the ensemble Kalman filter and how well does it work? *Proceedings of the 2006 American Control Conference Minneapolis*, Minnesota, USA, June 14–16, 2006. <https://ieeexplore.ieee.org/document/1657419>.
- GILLJNS, S., MENDOZA, O. B., CHANDRASEKAR, J., DE MOOR, B. L. R., BERNSTEIN, D. S. & RIDLEY, A. (2006a) What is the ensemble Kalman filter and how well does it work? *Proceedings of the 2006 American Control Conference Minneapolis*. Minnesota, USA, June 14–16.
- GIORDANO, G., BLANCHINI, F., BRUNO, R., COLANERI, P., DI FILIPPO, A., DI MATTEO, A. & COLANERI, M. (2020) Modelling the COVID-19 epidemic and implementation of population-wide interventions in Italy. *Nat. Med.*, **26**, 855–860. <https://doi.org/10.1038/s41591-020-0883-7>.
- GORBALENYA, A. E., BAKER, S. C., BARIC, R. S., et al. (2020) Severe acute respiratory syndrome-related coronavirus: the species and its viruses? A statement of the Coronavirus Study Group. Feb 11, 2020.
- GRIETTE, Q., MAGAL, P. & SEYDI, O. (2020) Unreported cases for age dependent COVID-19 outbreak in Japan. *Biology*, **9**, 132. <https://doi.org/10.3390/biology9060132>.

- GUAN, W.-J., CHEN, R.-C. & ZHONG, N.-S. (2020) Strategies for the prevention and management of coronavirus disease 2019. *Eur. Respir. J.*, **55**, 2000597.
- HEALTH, AFRICA (2020) *Latest on coronavirus outbreak*. Cameroon confirms first coronavirus case. <https://www.aa.com.tr/en/africa/cameroon-confirms-first-coronavirus-case/1756866>. March 6, 2020.
- HUANG, C., WANG, Y., LI, X., REN, L., ZHAO, J., HU, Y., ZHANG, L., FAN, G., XU, J., GU, X., CHENG, Z., YU, T., XIA, J., WEI, Y., WU, W., XIE, X., YIN, W., LI, H., LIU, M., XIAO, Y., GAO, H., GUO, L., XIE, J., WANG, G., JIANG, R., GAO, Z., JIN, Q., WANG, J. & CAO, B. (2020) Clinical features of patients infected with 2019 novel coronavirus in Wuhan, China. *Lancet*, **395**, 497–506.
- HUI, D. S., AZHAR, E. I. MADANI, T. A., NTOUMI, F., KOCK, R., et al. (2020a) The continuing 2019-nCoV epidemic threat of novel coronaviruses to global health? The latest 2019 novel coronavirus outbreak in Wuhan, China. Feb 01, 2020a, 264–266.
- HUI, D. S., AZHAR, E. I. MADANI, T. A., NTOUMI, F., KOCK, R., et al. (2020b) The continuing 2019-nCoV epidemic threat of novel coronaviruses to global health? The latest 2019 novel coronavirus outbreak in Wuhan, China. Feb 01, 2020, 264–266.
- HUSSEN H, ALEMU ZA. Risk of COVID-19 infection and associated factors among healthcare workers: a cross-sectional study at Eka Kotebe Treatment Center in Ethiopia. *Int. J. Gen. Med.*, 2021, 1763–1772. <https://doi.org/10.2147/IJGM.S301518>.
- KAILATH, T., SAYED, A. H. & HASSIBI, B. (2000) *Linear Estimation*. New Jersey: Prentice Hall, Inc.
- KAMPF, G., TODT, D., PFAENDER, S. & STEINMANN, E. (2020) Persistence of coronaviruses on inanimate surfaces and their inactivation with biocidal agents. *J. Hosp. Infect.*, **104**, 246–251.
- KAPEPULA, P. M., KABENGELE, J. K., KINGOMBE, M., VAN BAMBEKE, F., TULKENS, P. M., SADIKI KISHABONGO, A., DECLOEDT, E., ZUMLA, A., TIBERI, S., SULEMAN, F., TSHILOLO, L. MUYEMBE-TAMFUM, J. J., ZUMLA, A. & NACHEGA, J. B. (2020) Artemisia Spp. derivatives for COVID-19 treatment: anecdotal use, political hype, treatment potential, challenges, and road map to randomized clinical trials. *Amer. J. Trop. Med. Hygiene*, **103**, 960–964. <https://doi.org/10.4269/ajtmh.20-0820>.
- KOTECHA, J. H. & DJURIC, P. M. (2003) Gaussian particle filtering. *IEEE Trans. Signal Process.*, **51**, 2592–2601.
- LI, L., YANG, Z., DANG, Z., MENG, C., HUANG, J., MENG, H., WANG, D., CHEN, G., ZHANG, J., PENG, H. & SHAO, Y. (2020c) Propagation analysis and prediction of the COVID-19. *Infect. Dis. Model.*, **5**, 282–292.
- LI, Q., GUAN, X., WU, P., et al. (2020a) Early transmission dynamics in Wuhan, China, of novel coronavirus-infected pneumonia. *N. Engl. J. Med.*, Jan 29, 2020.
- LI, Y., WANG, B., PENG, R., ZHOU, C., ZHAN, Y., LIU, Z., JIANG, X. & ZHAO, B. (2020) Mathematical modeling and epidemic prediction of COVID-19 and its significance to epidemic prevention and control measures. *Ann. Infect. Dis. Epidemiol.*, **5**, 1052.
- LIN, Q., ZHAO, S., GAO, D., LOU, Y., YANG, S., MUSA, S. S., WANG, M. H., CAI, Y., WANG, W., YANG, L. & HE, D. (2020) A conceptual model for the coronavirus disease 2019 (COVID-19) outbreak in Wuhan, China with individual reaction and governmental action. *Int. J. Infect. Dis.*, **93**, 211–216.
- LIU, L., BAO, S., HU, T., WU, H., PENG, Z. & WANG, R. (2020) Estimating unreported COVID-19 cases in the United States based on time-varying SIR model. Available at <http://dx.doi.org/10.2139/ssrn.3691372>.
- LIU, Z., MAGAL, P. & WEBB, G. (2021) Predicting the number of reported and unreported cases for the COVID-19 epidemics in China, South Korea, Italy, France, Germany and United Kingdom. *J. Theor. Biol.*, **509**, 11050, in press. <https://doi.org/10.1016/j.jtbi.2020.110501>.
- MANAOUA, M. (2020) <https://twitter.com/DrManaouda/status/1286391057295577095>. July 23, 2020.
- MAUGERI, A., BARCHITTA, M., BATTIATO, S. & AGODI, A. (2020) Estimation of unreported novel coronavirus (SARS-CoV-2) infections from reported deaths: a susceptible-exposed-infectious-recovered-dead model. *J. Clin. Med.*, **9**, 1350. [10.3390/jcm9051350](https://doi.org/10.3390/jcm9051350).
- MBOPI-KEOU, F.-X., PONDI, J.-E. & SOSSO, M. A. (2020) COVID-19 in Cameroon: a crucial equation to resolve. *Lancet Infect. Dis.*, 1–1.
- MORADKHANI, H., SOROOSHIAN, S., GUPTA, H. V. & HOUSER, P. R. (2005) Dual state parameter estimation of hydrological models using ensemble Kalman filter. *Adv. Water Resour.*, **28**, 135–147.

- NADIM, S. S., GHOSH, I. & CHATTOPADHYAY, J. (2021) Short-term predictions and prevention strategies for COVID-19: a model-based study. *Appl. Math. Comput.*, **404**, 126251. <http://dx.doi.org/10.1016/j.amc.2021.126251>.
- NARULA, P., PIRATLA, V., BANSAL, A., AZAD, S. & LIO, P. (2016) Parameter estimation of tuberculosis transmission model using Ensemble Kalman filter across Indian states and union territories. *Infect. Dis. Health*, **21**, 184–191.
- NKWAYEP, C. H., BOWONG, S., TEWA, J. J. & KURTHS, J. (2020) Short-term forecasts of the COVID-19 pandemic: a study case of Cameroon. *Chaos Solitons Fractals*, **140**, 110106.
- PERKINS, T. A., CAVANY, S. M., MOORE, S. M., OIDTMAN, R. J., LERCH, A. & POTEREK, M. (2020) Estimating unobserved SARS-CoV-2 infections in the United States. *PNAS* **117**, 22597–22602, <https://doi.org/10.1073/pnas.2005476117>
- Perspective Monde (2020) <https://perspective.usherbrooke.ca/bilan/tend/CMR/fr/SP.DYN.LE00.IN.html> “Immunity passports” in the context of COVID-19. Scientific Brief.
- PHELAN, A. L., KATZ, R. & GOSTIN, L. (2020) The novel coronavirus originating in Wuhan, China: challenges for global health governance. Jan 30, 2020.
- Politologue.com (2020) *Evolution du Coronavirus (Covid19)*. <https://coronavirus.politologue.com/>. Update on July 04, 2021 and visited July 04, 2020.
- PREM, K., LIU, Y., RUSSELL, T. W., KUCHARSKI, A. J., EGGO, R. M., DAVIES, N., JIT, M., KLEPAC, P., FLASCHE, S., CLIFFORD, S., PEARSON, C. A. B., MUNDAY, J. D., ABBOTT, S., GIBBS, H., ROSELLO, A., QUILTY, B. J., JOMBART, T., SUN, F., DIAMOND, C., GIMMA, A., VAN ZANDVOORT, K., FUNK, S., JARVIS, C. I., EDMUNDS, W. J., BOSSE, N. I. & HELLEWELL, J. (2020) The effect of control strategies to reduce social mixing on outcomes of the COVID-19 epidemic in Wuhan, China: a modelling study. *Lancet Infect. Dis.*, **5**, 261–270.
- RANJAN, R. (2020) Predictions for COVID-19 outbreak in India using epidemiological models. April 12, 2020.
- ROCCHETTI, I., BÖHNING, D., HOLLING, H. & MARUOTTI, A. (2020) Estimating the size of undetected cases of the COVID-19 outbreak in Europe: an upper bound estimator. *Epidemiol. Methods*, **9**. <https://doi.org/10.1515/em-2020-0024>.
- RODA, W. C., VARUGHESE, M. B., HAN, D. & LI, M. Y. (2020) Why is it difficult to accurately predict the COVID-19 epidemic? *Infect. Dis. Model.*, **5**, 271–281.
- SALDAÑA, F., FLORES-ARGUEDAS, H., CAMACHO-GUTIÉRREZ, J. & BARRADAS, I. (2020) Modeling the transmission dynamics and the impact of the control interventions for the COVID-19 epidemic outbreak. *Mathematical Biosciences and Engineering*, **17**, 4165–4183. <https://doi.org/10.3934/mbe.2020231>.
- SONG, J., XIE, H., GAO, B., ZHONG, Y., GU, C. & CHOI, K.-S. (2021) Maximum likelihood-based extended Kalman filter for COVID-19 prediction. *Chaos Solitons Fractals*, **146**. <https://doi.org/10.1016/j.chaos.2021.110922>.
- Support the Guardian (2021) Immunity to Covid-19 could be lost in months, UK study suggests. <https://www.theguardian.com/world/2020/jul/12/immunity-to-covid-19-could-be-lost-in-months-uk-study-suggests>. July 12, 2020. Visited on July 01, 2021.
- TANG, B., BRAGAZZI, N. L., LI, Q., TANG, S., XIAO, Y. & WU, J. (2020) An updated estimation of the risk of transmission of the novel coronavirus (2019-nCov). *Infect. Dis. Model.*, **5**, 248–255.
- UNICEF (2020) Coronavirus? Gabon: UNICEF Gabon COVID-19 Situation Report. <https://reliefweb.int/report/gabon/unicef-gabon-covid-19-situation-report-no-6-10-26-june-2020>. Updated on June 26, 2020.
- UNICEF (2020) Gabon COVID-19 Situation Report No. 3: 1–16 May 2020. <https://reliefweb.int/report/gabon/unicef-gabon-covid-19-situation-report-no-3-1-16-may-2020>. Published on 16 May 2020 and visited July, 20, 2020.
- UNICEF (2020) Social stigma associated with the coronavirus disease (COVID-19). <https://www.unicef.org/documents/social-stigma-associated-coronavirus-disease-covid-19>. February 2020.
- VAN DEN DRIESSCHE, P. & WATMOUGH, J. (2002) Reproduction numbers and sub-threshold endemic equilibria for compartmental models of disease transmission. *Math. Biosci. Eng.*, **180**, 29–48.
- VERITY, R., OKELL, L. C., DORIGATTI, I., WINSKILL, P., WHITTAKER, C., IMAI, N., CUOMO-DANNENBURG, G., THOMPSON, H., WALKER, P. G. T., FU, H., DIGHE, A., GRIFFIN, J. T., BAGUELIN, M., BHATIA, S., BOONYASIRI, A., CORI, A., CUCUNUBÁ, Z., FITZJOHN, R., GAYTHORPE, K., GREEN, W., HAMLET, A., HINSLEY, W., LAYDON,

- D., NEDJATI-GILANI, G., RILEY, S., VAN ELSLAND, S., VOLZ, E., WANG, H., WANG, Y., XI, X., DONNELLY, C. A., GHANI, A. C. & FERGUSON, N. M. (2020) Estimates of the severity of coronavirus disease 2019: a model-based analysis. *Lancet Infect. Dis.* **20**, 669–677.
- WAN, E. A. & VAN DER MERWE, R. (2000) The unscented Kalman filter for nonlinear estimation. *Proc. The IEEE AS-SPCC Symposium*.
- WANG, D., HU, B., HU, C., ZHU, F., LIU, X., ZHANG, J., WANG, B., XIANG, H., CHENG, Z., XIONG, Y., ZHAO, Y., LI, Y., WANG, X. & PENG, Z. (2020) Clinical characteristics of 138 hospitalized patients with 2019 novel coronavirus-infected pneumonia in Wuhan, China. *JAMA*, Feb 7, 2020.
- WHO (2020) Transmission of SARS-CoV-2: implications for infection prevention precautions. July 9, 2020.
- WHO (2020) WHO supports scientifically-proven traditional medicine. <https://www.afro.who.int/news/who-supports-scientificallly-proven-traditional-medicine>. May 2020.
- WHO (2021) Press briefing variant on COVID-19. <https://www.afro.who.int/fr/node/12206>. Visited on July 2021.
- World Health Organisation (WHO) (2021) "Immunity passports" in the context of COVID-19. <https://www.who.int/news-room/commentaries/detail/immunity-passports-in-the-context-of-covid-19>, April 2020.
- WORLDOMETER (2020) COVID-19 CORONAVIRUS PANDEMIC. <https://www.worldometers.info/coronavirus/#countries>. Update on July 04, 2021 and visited July 04, 2020.
- ZHENG, D. Q., LEUNG, J. K. C. & LEE, B. Y. (2009) Online update of model state and parameters of a Monte Carlo atmospheric dispersion model by using ensemble Kalman filter. *Atmospher. Environ.*, **43**, 2005–2011.
- ZHOU, X., MA, X., HONG, N., SU, L., MA, Y., HE, J., JIANG, H., LIU, C., SHAN, G., ZHU, W., ZHANG, S. & LONG, Y. (2020) Forecasting the worldwide spread of COVID-19 based on logistic model and SEIR model. Adhikari et al. *Infect. Dis. Poverty*, 9–29.

Appendix A: Ensemble Kalman filter approach

Herein, we use the *EnKf* procedure (Bourgeois *et al.*, 2011; Gillijns *et al.*, 2006) to estimate the states x_t and the unknown parameters ϕ_t of l system (18) for each data \mathcal{Y}_t using the following system:

$$\begin{cases} x_{t+1} = f(x_t, \phi_t, u_t) + w_t, \\ \mathcal{Y}_t = h(x_t, \phi_t) + \psi_t, \\ \phi_{t+1} = \phi_t + \sigma_t. \end{cases} \quad (18)$$

The estimate state-parameter mechanism of Eq. (18) is based on a prediction-correction scheme for the state x_t and the parameter ϕ_t at time t .

We begin by the design of estimating the state. In the forecast step, we prepare both of the ensemble of n forecasted states with random sampling error and the set of predicted outputs as

$$x_{t+1}^{fi} = f(x_t^{ai}, \phi_t^a, u_t) + w_t^i \quad \text{and} \quad \mathcal{Y}_{t+1}^{fi} = h(x_{t+1}^{fi}, \phi_t^a), \quad i = 1, 2, \dots, n, \quad (19)$$

where the superscript fi refers to the i -th member of the ensemble of data, ϕ_t^a is the estimate value of ϕ_t at time t and the vector x_t^{ai} corresponds to the i -th member of the set of states corrected at the moment t . Then, for the step of correction, the set means defined as \bar{x}_{t+1}^f and $\bar{\mathcal{Y}}_{t+1}^f$ are respectively given by

$$\bar{x}_{t+1}^f = \frac{1}{n} \sum_{i=1}^n x_{t+1}^{fi} \quad \text{and} \quad \bar{\mathcal{Y}}_{t+1}^f = \frac{1}{n} \sum_{i=1}^n \mathcal{Y}_{t+1}^{fi}. \quad (20)$$

Thus, the forecast ensemble mean, which is the best forecast estimate of the state, and the spread of the ensemble members around the mean as the error between the best estimate and the actual state by

$$R_{t+1} = \frac{1}{n-1} \sum_{i=1}^n v_{t+1}^i (v_{t+1}^i)^T. \quad (21)$$

Thus, the covariance matrices of the error at time $t + 1$ are

$$P_{x\mathcal{Y},t+1} = \frac{1}{n-1} \sum_{i=1}^n E_{x,t+1}^{fi} (E_{\mathcal{Y},t+1}^{fi})^T \quad \text{and} \quad P_{y\mathcal{Y},t+1} = \frac{1}{n-1} \sum_{i=1}^n E_{\mathcal{Y},t+1}^{fi} (E_{\mathcal{Y},t+1}^{fi})^T, \quad (22)$$

where $E_{x,t+1}^{fi} = x_{t+1}^{fi} - \bar{x}_{t+1}^f$ and $E_{\mathcal{Y},t+1}^{fi} = \mathcal{Y}_{t+1}^{fi} - \bar{\mathcal{Y}}_{t+1}^f$.

$P_{x\mathcal{Y},t+1}$ is the unbiased empirical estimator of the covariance matrix of the cross-prediction error between the state and the output at time $t + 1$. Similarly, $P_{y\mathcal{Y},t+1}$ represents the unbiased estimator of the covariance matrix of the prediction error of the output at time $t + 1$.

The second step is the analysis. To obtain the estimate analysis of the state, the *EnKf* performs an ensemble of parallel data assimilation cycles. This step consists of updating each available member of the set of draft states using the current observation. For this, the following linear correction equation is applied

$$x_{t+1}^{ai} = \bar{x}_{t+1}^{fi} + K_{t+1} (\mathcal{Y}_{t+1} + v_{t+1}^i - \mathcal{Y}_{t+1}^{fi}), \quad i = 1, 2, \dots, n, \quad (23)$$

where K_{t+1} is the Ensemble Kalman filter gain is defined as

$$K_{t+1} = P_{x\mathcal{Y},t+1} (P_{y\mathcal{Y},t+1} + R_{t+1})^{-1}. \quad (24)$$

Finally, the estimate state of x_{t+1} is the mean of all estimation x_{t+1}^{ai} defined as follows:

$$x_{t+1}^a = \frac{1}{n} \sum_{i=1}^n x_{t+1}^{ai}. \quad (25)$$

The second design concerns the estimation β_{t+1}^a of the vector of parameters ϕ_{t+1} at time $t + 1$.

As at the state estimation, we prepare the ensemble of N forecasted states with random sampling error as

$$\phi_{t+1}^{fi} = \phi_t^{fi} + \phi_t^i, \quad i = 1, 2, \dots, n. \quad (26)$$

The ensemble mean is defined as

$$\bar{\phi}_{t+1}^f = \frac{1}{n} \sum_{i=1}^n \phi_{t+1}^{fi}. \quad (27)$$

The ensemble error matrix for the state variable is defined as follows:

$$E_{\phi,t+1}^{fi} = \phi_{t+1}^{fi} - \bar{\phi}_{t+1}^f, \quad i = 1, \dots, n. \quad (28)$$

and the ensemble error matrix for the observed variables is defined as follows:

$$E_{\mathcal{Y},t+1}^{fi} = \mathcal{Y}_{t+1}^{\phi fi} - \bar{\mathcal{Y}}_{t+1}^{ff}, \quad i = 1, 2, \dots, n, \quad (29)$$

where $\mathcal{Y}_{t+1}^{\phi fi} = h(x_{t+1}^a, \phi_{t+1}^{fi})$ $i = 1, 2, \dots, n$.

For the analysis steps, the Kalman gain matrix of $EnKf$ K_{t+1} is

$$K_{\beta,t+1} = P_{\phi\mathcal{Y},t+1} (P_{\phi\mathcal{Y}\mathcal{Y},t+1} + R_{t+1})^{-1}, \quad (30)$$

where the error covariance matrices $P_{\phi\mathcal{Y},t+1}$ and $P_{\phi\mathcal{Y}\mathcal{Y},t+1}$ are given by

$$P_{\phi\mathcal{Y},t+1} = \frac{1}{n-1} \sum_{i=1}^n E_{\phi,t+1}^{fi} (E_{\mathcal{Y},t+1}^{fi})^T \text{ and } P_{\phi\mathcal{Y}\mathcal{Y},t+1} = \frac{1}{n-1} \sum_{i=1}^n E_{\phi\mathcal{Y}\mathcal{Y},t+1}^{fi} (E_{\mathcal{Y}\mathcal{Y},t+1}^{fi})^T. \quad (31)$$

Appendix B: Proof of the basic properties of system (4)

In this Appendix, we prove that any solution of system (4) with a positive initial condition remains positive and bounded. The proof is done in two steps.

Step 1: We show that the solution $X(t)$ of system (4) corresponding to initial conditions such that $X(0) > 0$ are nonnegative for all $t > 0$.

Suppose that $X(0) > 0$. Then from the model equation and properties of continuous functions, there exists some $t_0 > 0$ so that $X(t)$ remains non-negative for all $t \in]0, t_0[$. We are now going to show that $t_0 = \infty$.

Suppose that $t_0 < \infty$. Hence, there exists $t_1 \geq t_0$, which vanish at least one component of X . We define

$$t^* = \inf\{t_1 \geq t_0 : S_u(t_1) = 0 \text{ or } S_a(t_1) = 0 \text{ or } I_d(t_1) = 0 \text{ or } I_u(t_1) = 0 \text{ or } R(t_1) = 0 \text{ or } V(t_1) = 0\}.$$

Suppose that $S_u(t_1) = 0$ and let us consider the first equation of system (4):

$$\dot{S}_u(t) = \Lambda + \gamma S_a(t) - (\lambda + \rho + \mu) S_u(t).$$

From the above equation, one has that

$$\dot{S}_u(t) + (\lambda + \rho + \mu) S_u(t) > 0.$$

Integrating the above inequality from 0 to t^* , one can deduce that

$$\int_0^{t^*} \frac{d}{dt} \left[S_u(t) \exp \left(\int_0^t \lambda(s) ds + (\rho + \mu)t \right) \right] > 0.$$

Since $S(0) > 0$, one has that

$$S_u(t^*) > S_u(0) \exp\left(-\int_0^{t^*} \lambda(s) ds - (\rho + \mu)t^*\right) > 0,$$

which is a contradiction with the fact that $S_u(t^*) = 0$. Using the same arguments, we prove by the absurdity of $t_0 < \infty$ that $S_d(t^*) > 0$, $I_d(t^*) > 0$, $I_u(t^*) > 0$, $R(t^*) > 0$ and $V(t^*) > 0$. Therefore, the trajectories of the solutions of system (4) remain positive for all $t \in [0, +\infty[$.

Step 2: We prove that the total population human and the free SARS-CoV-2 in the environment at time t , $N(t)$ and $V(t)$ are bounded.

1. Adding the fifth first equations in system (4), the dynamics of total human population satisfies

$$\dot{N}(t) = \Lambda - \mu N(t) - d_d I_d(t) - d_u I_u(t) \leq \Lambda - \mu N(t). \quad (32)$$

Applying the Gronwall inequality to the above differential inequality (32) yields

$$N(t) \leq \frac{\Lambda}{\mu} + \left(N(0) - \frac{\Lambda}{\mu}\right) e^{-\mu t}, \quad \forall t \geq 0, \quad (33)$$

where $N(0)$ represents the initial value of $N(t)$. Then, one can conclude that $N(t) \leq \frac{\Lambda}{\mu}$ for all time $t \geq 0$ if $N(0) \leq \frac{\Lambda}{\mu}$.

2. Finally, using the last equation of system (4) and the fact that $I_d(t)$, $I_u(t) \leq \frac{\Lambda}{\mu}$ for all time $t \geq 0$, one obtains

$$\dot{V}(t) \leq \frac{(\xi_d + \xi_u)\Lambda}{\mu} - \nu_v V(t). \quad (34)$$

Applying again the Gronwall inequality to the above differential inequality (34), one has that

$$V(t) \leq \frac{(\xi_d + \xi_u)\Lambda}{\nu\mu}, \quad \text{for all } t \geq 0,$$

$$\text{if } V(0) \leq \frac{(\xi_d + \xi_u)\Lambda}{\nu\mu}.$$

Therefore, combining *Step 1* and *Step 2*, the results about the positivity and the boundedness of solutions are proved. This completes the proof. \square

Appendix C: Computation of the basic reproduction number \mathcal{R}_0 of system (4)

Herein, we show how to calculate the basic reproduction number \mathcal{R}_0 of system (4).

Using the notations in [Van den Driessche & Watmough \(2002\)](#) for system (4), the new infection term and the remaining transfer term are $\mathcal{F} = ((pS_u + q(1 - \eta)S_a)\lambda(I_u, I_d, V), ((1 - p)S_u + (1 - q)(1 - \eta)S_c)\lambda(I_u, I_d, V), 0)^T$ and $\mathcal{W} = (-\omega I_u + (d_d + \theta + \mu)I_d, (\delta + \omega(1 - \delta) + d_u + \mu)I_u, -\xi_u I_u - \xi_d I_d + \nu V)^T$, respectively. So, their Jacobian matrices evaluated at the DFE X_0 are given by linearizing \mathcal{F} and \mathcal{W} at X_0 and one has

$$F = \begin{bmatrix} \frac{\varepsilon\beta_h}{N^0}S^0 & \frac{\beta_h}{N^0}S^0 & \frac{\beta_v}{K}S^0 \\ \frac{\varepsilon\beta_h}{N^0}C^0 & \frac{\beta_h}{N^0}C^0 & \frac{\beta_v}{K}C^0 \\ 0 & 0 & 0 \end{bmatrix} \quad \text{and} \quad W = \begin{bmatrix} d_d + \theta + \mu & -\omega & 0 \\ 0 & \delta + \omega + d_u + \mu & 0 \\ -\xi_d & -\xi_u & \nu \end{bmatrix},$$

where $S^0 = (pS_u^0 + q(1 - \eta)S_a^0)$, $C^0 = ((1 - p)S_u^0 + (1 - q)(1 - \eta)S_a^0)$, $S_u^0 = \frac{(\gamma + \mu)\Lambda}{(\rho + \gamma + \mu)\mu}$ and $S_a^0 = \frac{\rho\Lambda}{(\rho + \gamma + \mu)\mu}$.

A simple computation gives

$$W^{-1} = \begin{bmatrix} \frac{1}{d_d + \theta + \mu} & \frac{\omega}{(d_d + \theta + \mu)(\delta + \omega + d_u + \mu)} & 0 \\ 0 & \frac{1}{\delta + \omega + d_u + \mu} & 0 \\ \frac{\xi_d}{(d_d + \theta + \mu)\nu} & \frac{\xi_u(d_d + \theta + \mu) + \xi_u\omega}{(d_d + \theta + \mu)(\delta + \omega + d_u + \mu)\nu} & \frac{1}{\nu} \end{bmatrix}.$$

Then, the basic reproduction number of system (4) is the maximum eigenvalue of the next generation matrix FW^{-1} given by

$$FW^{-1} = \begin{bmatrix} F_{11} & F_{12} & \frac{\beta_v S^0}{K\nu} \\ F_{21} & F_{22} & \frac{\beta_v C^0}{K\nu} \\ 0 & 0 & 0 \end{bmatrix},$$

where

$$\begin{aligned}
 F_{11} &= \left(\frac{\varepsilon\beta_h}{N^0} + \frac{\xi_d\beta_v}{Kv} \right) \frac{S^0}{d_d + \theta + \mu}, \\
 F_{21} &= \left(\frac{\varepsilon\beta_h}{N^0} + \frac{\xi_d\beta_v}{Kv} \right) \frac{C^0}{d_d + \theta + \mu}; \\
 F_{12} &= \left[\left(\frac{\omega\varepsilon}{d_d + \theta + \mu} + 1 \right) \frac{\beta_h}{N^0} + \beta_v \frac{\xi_u(d_d + \theta + \mu) + \xi_d\omega}{(d_d + \theta + \mu)Kv} \right] \frac{S^0}{\delta + \omega + d_u + \mu} \\
 F_{22} &= \left[\left(\frac{\omega\varepsilon}{d_d + \theta + \mu} + 1 \right) \frac{\beta_h}{N^0} + \beta_v \frac{\xi_u(d_d + \theta + \mu) + \xi_d\omega}{(d_d + \theta + \mu)Kv} \right] \frac{C^0}{\delta + \omega + d_u + \mu}.
 \end{aligned}$$

Since $F_{11}F_{22} - F_{12}F_{21} = 0$, the basic reproduction number of system (4) is

$$\mathcal{R}_0 = \mathcal{R}_{0h} + \mathcal{R}_{0v}, \quad (35)$$

where

$$\mathcal{R}_{0h} = \frac{\beta_h}{N^0} \left[\frac{\varepsilon S^0}{d_d + \theta + \mu} + \left(\frac{\omega\varepsilon}{d_d + \theta + \mu} + 1 \right) \frac{C^0}{\delta + \omega + d_u + \mu} \right]$$

and

$$\mathcal{R}_{0v} = \frac{\beta_v}{(d_d + \theta + \mu)Kv} \left(\xi_d S^0 + \frac{(\xi_u(d_d + \theta + \mu) + \xi_d\omega)C^0}{\delta + \omega + d_u + \mu} \right).$$

with S^0 , C^0 , S_u^0 and S_a^0 defined as in Eq. (9). □